Unclassified
SECURITY CLASSIFICATION OF THIS PAGE (When Data Entered)

(1)

REPORT DOCUMENTATION PAGE

READ INSTRUCTIONS BEFORE COMPLETING FORM

1. REPORT NUMBER	2. GOVT ACCESSION NO.	3. RECIPIENT'S CATALOG NUMBER
	AD-A134895	

4. TITLE (and Subtitle)

Body and Surface Wave Modeling of Observed Seismic Events

5. TYPE OF REPORT & PERIOD COVERED
Semi-Annual Technical Report
1 Oct.1977 - 31 Mar. 1978

6. PERFORMING ORG. REPORT NUMBER

7. AUTHOR(s)
David G. Harkrider
Donald V. Helmberger
J. Bernard Minster

8. CONTRACT OR GRANT NUMBER(s)
F49620-77-C-0022

9. PERFORMING ORGANIZATION NAME AND ADDRESS
California Institute of Technology
Seismological Laboratory
Pasadena, California 91125

10. PROGRAM ELEMENT, PROJECT, TASK AREA & WORK UNIT NUMBERS
ARPA Order 3291,Amendment 11
8F10

11. CONTROLLING OFFICE NAME AND ADDRESS
AFOSR
Building 410
Bolling AFB, D.C. 20332

12. REPORT DATE
April 25, 1978

13. NUMBER OF PAGES
75

14. MONITORING AGENCY NAME & ADDRESS(if different from Controlling Office)

15. SECURITY CLASS. (of this report)
Unclassified

15a. DECLASSIFICATION/DOWNGRADING SCHEDULE

16. DISTRIBUTION STATEMENT (of this Report)

Approved for public release; distribution unlimited

17. DISTRIBUTION STATEMENT (of the abstract entered in Block 20, if different from Report)

18. SUPPLEMENTARY NOTES

19. KEY WORDS (Continue on reverse side if necessary and identify by block number)

Explosion P waves
von Seggern-Blandford RDP
Amchitka-Novaya Zemlya events
Generalized ray and normal mode comparison
Near field & far field generalized ray approximations
Fault conversion to shear waves

20. ABSTRACT (Continue on reverse side if necessary and identify by block number)

The research completed under this contract during the period 1 October 1977 - 31 March 1978 falls within the two broad topics of (1) seismic source mechanisms and (2) seismic propagation structure and attenuation. These two topics are both relevant to the detection and discrimination of seismic events.

Using a deconvolution technique, which makes use of both the long and short period observations of body waves, a broad band deconvolved explosion

DD FORM 1 JAN 73 1473 EDITION OF 1 NOV 65 IS OBSOLETE

Unclassified
SECURITY CLASSIFICATION OF THIS PAGE (When Data Entered)

P wave is obtained. The early part of this signal is used to estimate the parameters of a vonSeggern-Blandford modification of the theoretical Haskell explosion RDP, which allows apparent discontinuities in source velocity and acceleration at the beginning of the RDP. Synthetic teleseismic P wave signals are obtained for this RDP at a shallow and deep source depth with a t* of 1 sec. Wave form comparisons with teleseismic short and long period observations of events from Amchitka and Novaya Zemlya are excellent. The primary theoretical difference between the comparison events in the two regions appears to be due to source depth.

In order to determine the correspondence between generalized ray and normal mode theory in the generation of Lg phase, we have begun a program of synthesizing seismograms for sources in simple plane layered models of the lithospheric wave guide using both generalized rays and normal modes. In this report we show synthetics for the fundamental and first five overtones of the Rayleigh and Love normal modes for a simple layer over a half space and compare them with generalized ray seismograms at various ranges. A comparison at 128 km for a far field trapezoid source history of $\delta t_1 = \delta t_2 = \delta t_3 = .2$ sec shows good agreement especially at longer periods. Because of the good agreement at long periods, we increased the source history duration to $\delta t_1 = \delta t_2 = \delta t_3 = .5$ sec and calculated SH comparisons at ranges if 100 km to 1000 km using 100 km increments. The agreement at all ranges is extremely good, especially in the relative arrival times of various body phases in the wave train. One of the unexpected results was that the direct SH wave received most of its contribution from the Love fundamental mode. In general, the higher the mode the later its contribution to the wave train.

The complete linear response of plane, elastic layered solid to a shear dislocation is investigated. The solution is expressed as a summation of generalized rays of the P, SV and SH potentials. This allows the transient response to be obtained upon application of the Cagniard-de Hoop technique. Numerical results of the full solution containing the near and far field terms are compared for a whole space, half space and layered model with asymptotic solutions to establish the advantages and limitations of approximate methods.

Because of the presence of large fault systems near NTS and the Sahara test sites, we have investigated the theoretical seismic radiation formed by an explosion in the vicinity of an infinite fault with various slip conditions. The results show that it is possible to generate S wave radiation by detonating an explosive P wave source near a vertical fault across which differential slip is allowed to occur. This mechanism does not require the existence of regional prestress, but will, in general, be quite inefficient unless the fault is fairly well lubricated. It must be noted that although the SH wave amplitude radiation pattern show a superficial resemblance to double couple radiation patterns, the phase is quite different in orientation about the fault plane.

Seismological Laboratory
Division of Geological and Planetary Sciences
California Institute of Technology
Pasadena, California 91125

SEMI-ANNUAL TECHNICAL REPORT

1 October 1977 - 31 March 1978

ARPA Order No.:	3291, Amendment 11
Program Code:	8F10
Name of Contractor:	California Institute of Technology
Effective Date of Contract:	1 October 1976
Contract Expiration Date:	30 September 1978
Amount of Contract:	$257,063
Contract Number:	F49620-77-C-0022
Principal Investigators and Telephone Numbers:	David G. Harkrider (213) 795-6811, Ext. 2910 Donald V. Helmberger (213) 795-6811, Ext. 2911 J. Bernard Minster (213) 795-6811, Ext. 2909
Program Manager and Telephone Number:	William J. Best (202) 767-5011
Short Title of Work:	Body and Surface Wave Modeling of Observed Seismic Events

Sponsored by
Advanced Research Projects Agency (DOD)
ARPA Order No. 3291, Amendment 11
Monitored by AFOSR Under Contract #F49620-77-C-0022

TABLE OF CONTENTS

I. Summary

The research completed under this contract during the period 1 October 1977 - 31 March 1978 falls within the two broad topics of (1) seismic source mechanisms and (2) seismic propagation structure and attenuation. These two topics are both relevant to the detection and discrimination of seismic events.

Using a deconvolution technique, which makes use of both the long and short period observations of body waves, a broad band deconvolved explosion P wave is obtained. The early part of this signal is used to estimate the parameters of a von Seggern-Blandford modification of the theoretical Haskell explosion RDP, which allows apparent discontinuities in source velocity and acceleration at the beginning of the RDP. Synthetic teleseismic P wave signals are obtained for this RDP at a shallow and a deep source depth with a t* of 1 sec. Wave form comparisons with teleseismic short and long period observations of events from Amchitka and Novaya Zemlya are excellent. The primary theoretical difference between the comparison events in the two regions appears to be due to source depth.

In order to determine the correspondence between generalized ray and normal mode theory in the generation of Lg phase, we have begun a program of synthesizing seismograms for sources in simple plane layered models of the lithospheric wave guide using both generalized rays and normal modes. In this report we show synthetics for the fundamental and first five overtones of the Rayleigh and Love normal modes for a simple layer over a half space and compare them with generalized ray seismograms at various ranges. A comparison at 128 kms for a far field trapezoid source history of

$\delta t_1 = \delta t_2 = \delta t_3 = .2$ secs shows good agreement especially at longer periods. Because of the good agreement at long periods, we increased the source history duration to $\delta t_1 = \delta t_2 = \delta t_3 = .5$ secs and calculated SH comparisons at ranges of 100 km to 1000 km using 100 km increments. The agreement at all ranges is extremely good, especially in the relative arrival times of various body phases in the wave train. One of the unexpected results was that the direct SH wave received most of its contribution from the Love fundamental mode. In general, the higher the mode the later its contribution to the wave train.

The complete linear response of plane, elastic layered solid to a shear dislocation is investigated. The solution is expressed as a summation of generalized rays of the P, SV and SH potentials. This allows the transient response to be obtained upon application of the Cagniard-de Hoop technique. Numerical results of the full solution containing the near and far field terms are compared for a whole space, half space and layered model with asymptotic solutions to establish the advantages and limitations of approximate methods.

Because of the presence of large fault systems near NTS and the Sahara test sites, we have investigated the theoretical seismic radiation formed by an explosion in the vicinity of an infinite fault with various slip conditions. The results show that it is possible to generate S wave radiation by detonating an explosive P wave source near a vertical fault across which differential slip is allowed to occur. This mechanism does not require the existence of regional prestress, but will, in general, be quite inefficient unless the fault is fairly well lubricated. It must be noted that although the SH wave amplitude radiation pattern show a superficial resemblance to

double couple radiation patterns, the phase is quite different in orientation about the fault plane.

II. Time Functions for Nuclear Explosions

L. J. Burdick and D. V. Helmberger

Introduction

In recent years the methods of computer synthesis of body waveforms have provided a wealth of information about earthquake sources and about earth structure. The same methods will almost certainbe be equally useful in the analysis of body waves from bombs, now that both short and long period data for large events has become available. A theoretical representation for the explosive source must be formulated which is both simple enough to be used easily and accurate enough to predict high frequency body waves. A number of possible representations have been proposed. Haskell (1967) devised a form for the bomb time function by assuming the boundary conditions at the source and fitting some observed Fourier amplitude spectra. Helmberger and Harkrider (1971) pointed out that the rise time was too slow in Haskell's model and importance of overshoot in the long period LRSM data. More recently, von Seggern and Blandford (1972), used a simplified form of Haskell's expression allowing a faster rise time and modeled the Amchitka short period data using spectral methods. This last formulation is the one which will be discussed here since it is the simplest. However, the free parameters in the expression for the bomb time function will be reevaluated since the requirements for a theoretical time function in a synthetic seismogram calculation involving both short and long periods are particularly demanding.

METHODS

The approach used in modeling the explosive time function was to assume that all of the methods for modeling earthquake waveforms carry over to the explosive source case. Thus, the synthetic seismograms were represented as successive convolutions of an instrument operator, a Futterman Operator evaluated at a t* of 1.0 and a free surface (P + pP) operator. As usual, the mantle and receiver responses were assumed to be delta functions for the ranger from 30° to 90°. The bomb source time function was constrained by trial and error modeling of waveform and amplitude data from both the Amchitka and the Novaya Zemlyz test sites. In order to eliminate some of the difficulty in the trial and error process of finding a time function, the relatively stable instrument and Q operator were deconvolved from some good quality observed records. The von Seggern and Blandford time function was used to fit the resulting pulse. A full synthetic seismogram calculation was then carried out, and the source was adjusted until a reasonable fit to the data was achieved.

Analysis and Results

The deconvolution procedure used to establish the bomb time function convolved with the free surface operator is the one discussed by Burdick and Mellman (1976). It involves using both a WWSSN short period record and a WWSSN long period record of a pulse to obtain a composite, broad-band deconvolved pulse which is compatible with both. Figure 1 (top) shows the deconvolved pulse for a Novaya Zemlya event as observed at ATL. Several observed records from Novaya Zemlya events are shown next and at the bottom is the result obtained when the deconvolved pulse is convolved with a long

with a long or a short period instrument. The good correspondence between the observed and synthetic records demonstrates that the deconvolved source is a good estimate of the time function-free surface pulse from Novaya Zemlyz. An interesting aspect of the result is that the downswing in the source pulse is slightly larger than the upswing. This is difficult to understand since the downswing must be primarily pP which must be smaller than P. Figure 2 shows that this effect can be explained if the source time function is allowed to be two-sided. This corresponds to allowing B to be greater than zero in von Seggern and Blandford's expressions. The reduced displacement potentials for a number of B values are shown on the left of Figure 2. Note the increase in overshoot which corresponds to a negative overswing in the time function or B is increased. On the right of Figure 2 is a comparison of the far field time function for the displacement potentials with the deconvolved pulse. The time functions have been convolved with a free surface operator, so they should correspond directly with the deconvolved pulse. The best fit occurs for a B value of about 2 to 5 which corresponds to a 2:1 or 3:1 overshoot in the potential. The value of K which controls the rise time in the formulation was set at 5 sec^{-1}.

Figure 3 compares fully theoretical seismograms computed with the von Seggern and Blandford source with some additional Novaya Zemlya data. The synthetics are computed for the case of a deep source (P - pP time = 1 sec) and a shallow source (P - pP time - .5 sec). The short period records shown in the figure were from smaller bombs, so they fit the shallow event synthetics. The long period records shown were from large bombs and they correspond better with the deep source synthetics. The implication is that the main differences in waveshape between big and small bombs are caused by

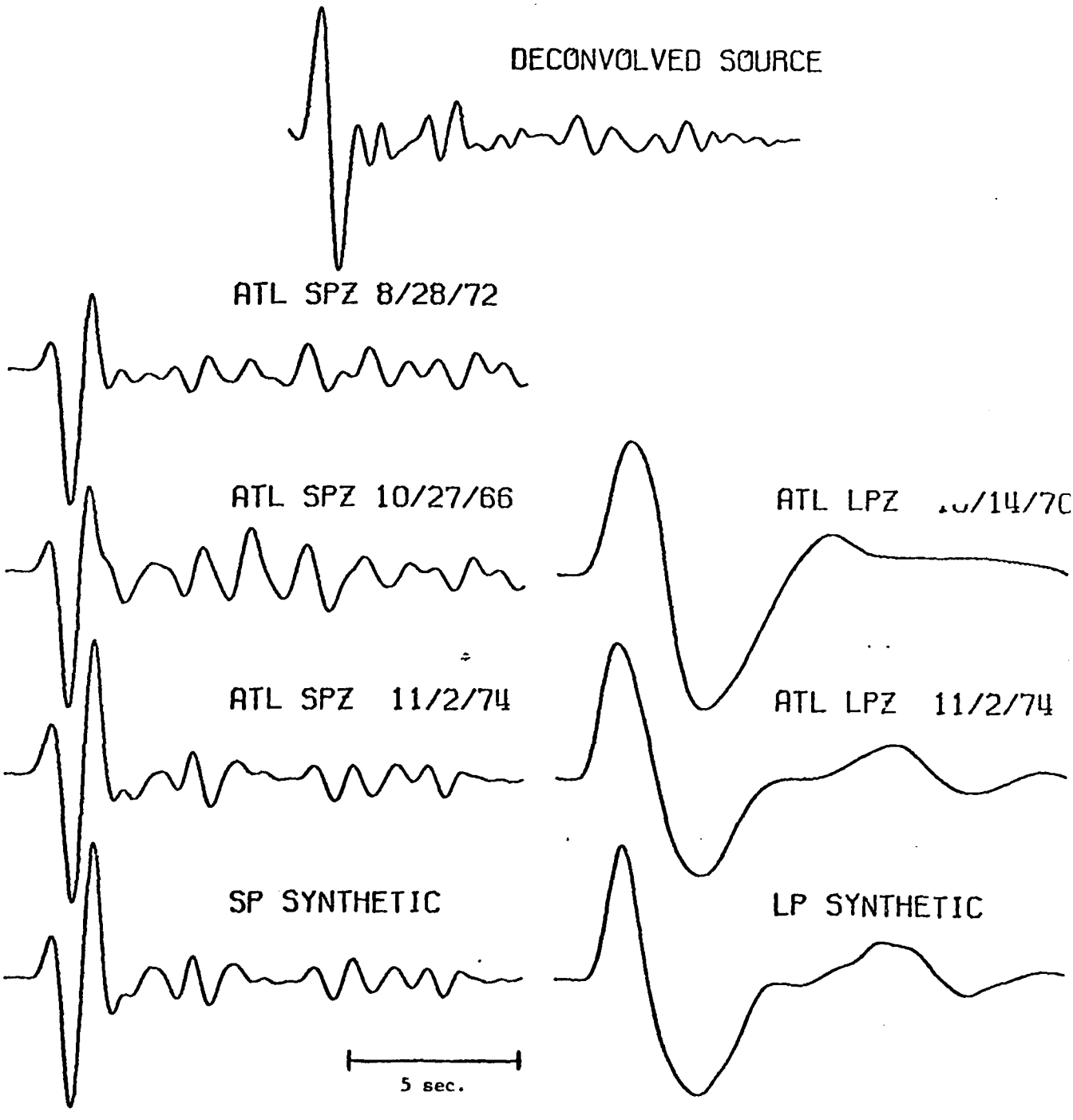
DECONVOLVED SOURCE
ATL SPZ 8/28/72
ATL SPZ 10/27/66
ATL LPZ
ATL SPZ 11/2/74
ATL LPZ 11/2/74
SP SYNTHETIC
LP SYNTHETIC
5 sec.

Figure II-1

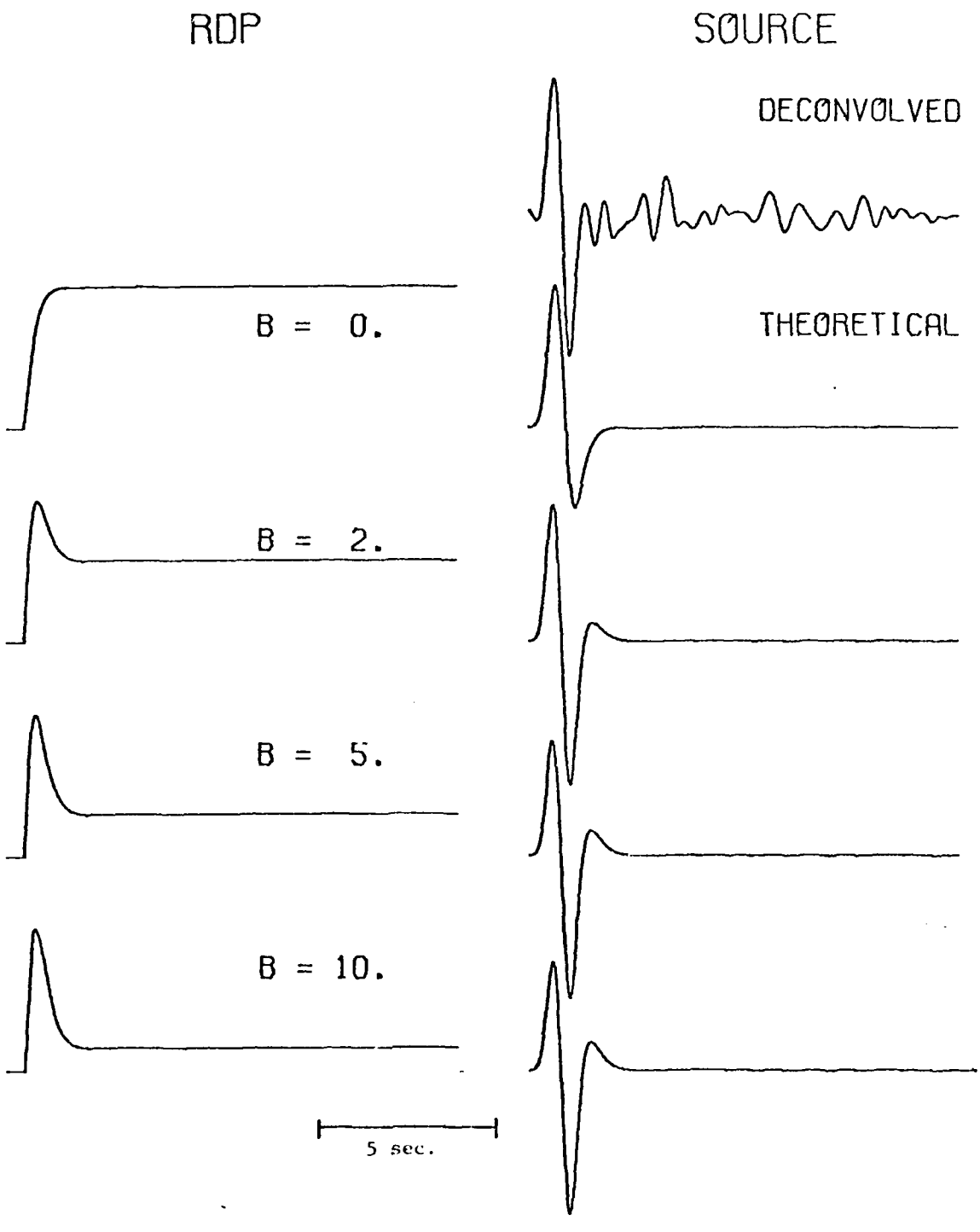

Figure II-2

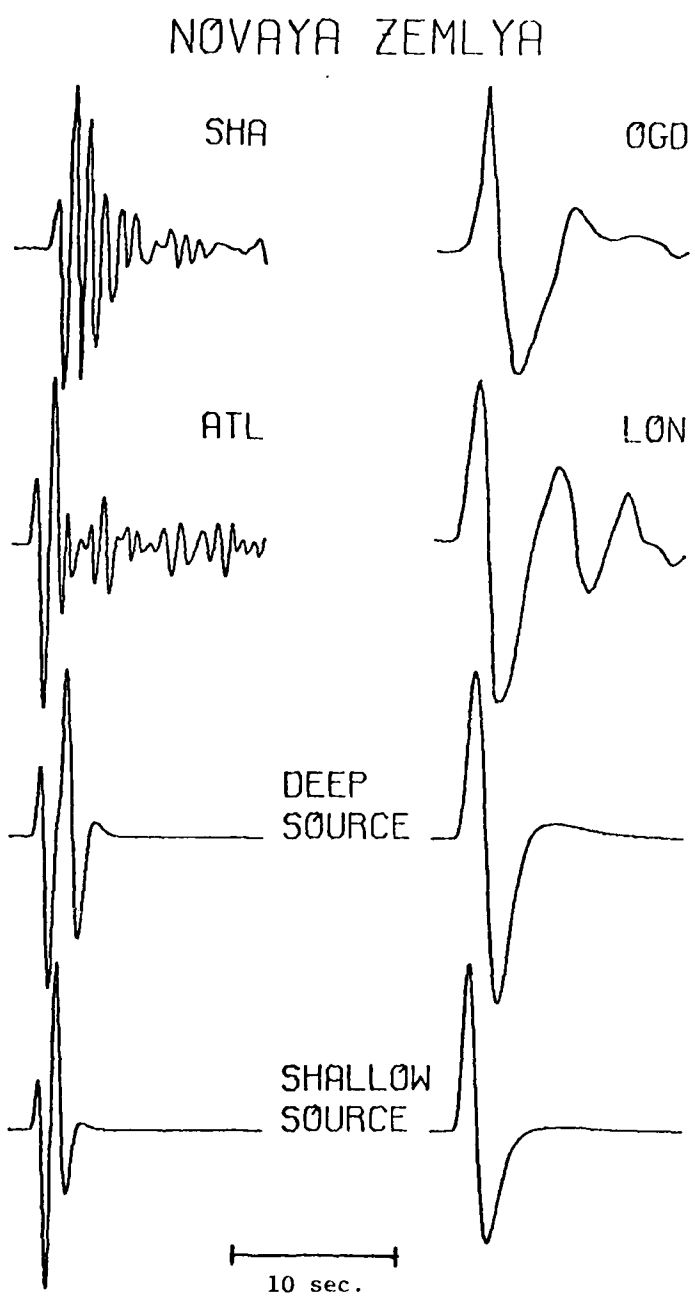
NOVAYA ZEMLYA
SHA
OGD
ATL
LON
DEEP
SOURCE
SHALLOW
SOURCE
10 sec.

Figure II-3

a difference in source depth. Undoubtedly source shape changes with event size as well, but this effect is small compared to the depth effect. It would be of great interest to try the source model for simultaneous short and long period records of a bomb, but the WWSSN gains are set so these types of records are rare. If the long period record is sufficiently large, the short period record is usually off scale.

Figure 4 shows a comparison of data and synthetics for the Amchitka blast, Cannikin. This event was so deep that the pP appears as a visible feature in the short period records. This feature is predicted very accurately by the synthetics. The long period records show a peculiar double backswing which is only weakly present in the synthetics. However, the double backswing is caused by the interaction of the time function with the near source velocity structure and it is very difficult to model without precise knowledge of this structure. The important point is that again varying just the depth explains most of the observed data.

Figure 5 shows a comparison of the observed versus computed short period to long period amplitude ratios for Cannikin and Novaya Zemlya. The Novaya Zemlya data is again almost all from small events. The observed ratio is predicted if a short P - pP time is used in the synthetic. If a longer time is used one predicts the long period-short period ratio observed for Cannikin.

Conclusions

It has been shown that for appropriate choices of the parameters in the von Seggern and Blandford source description it is possible to fit a number of teleseismic body wave observations. These include the long period

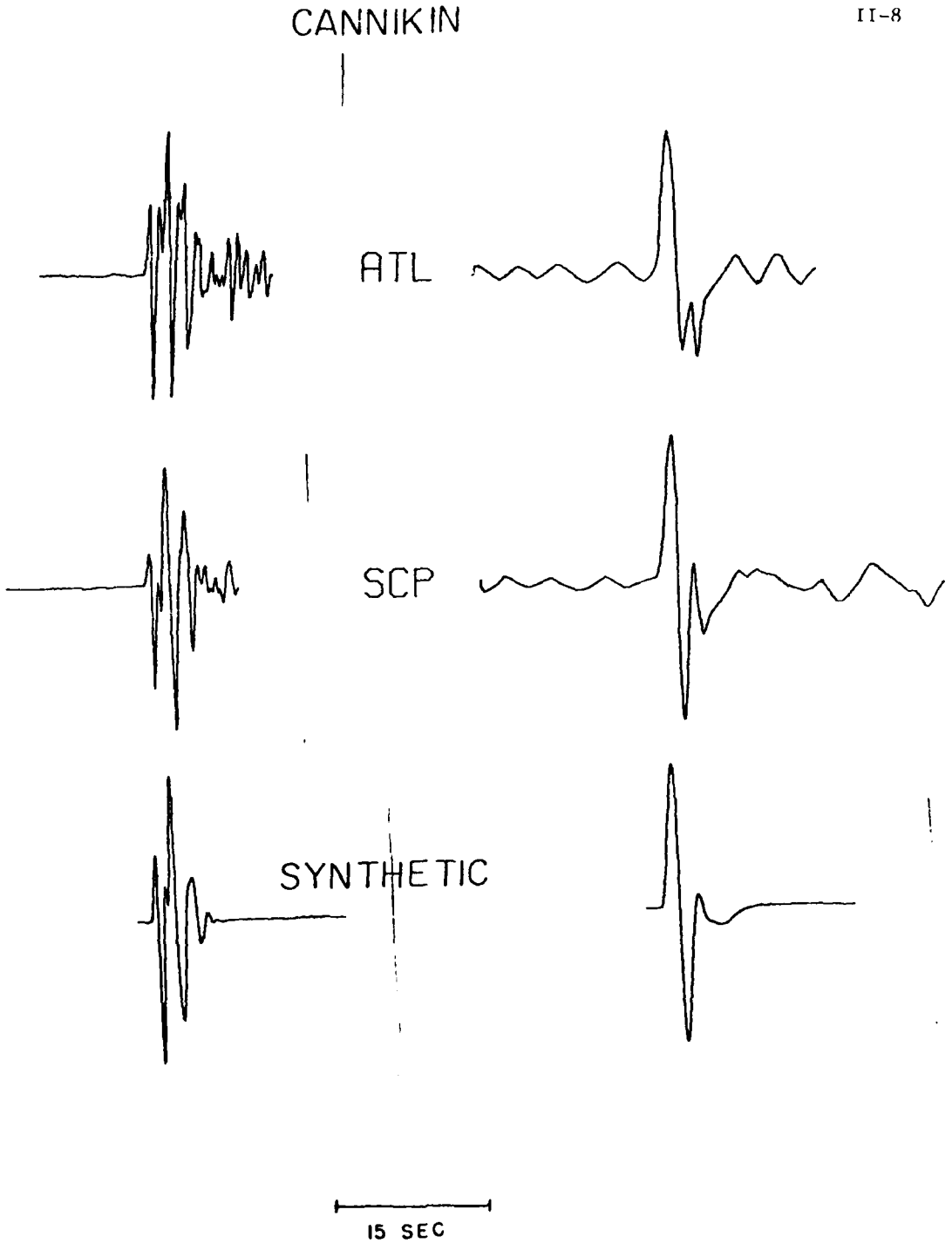

Figure II-4

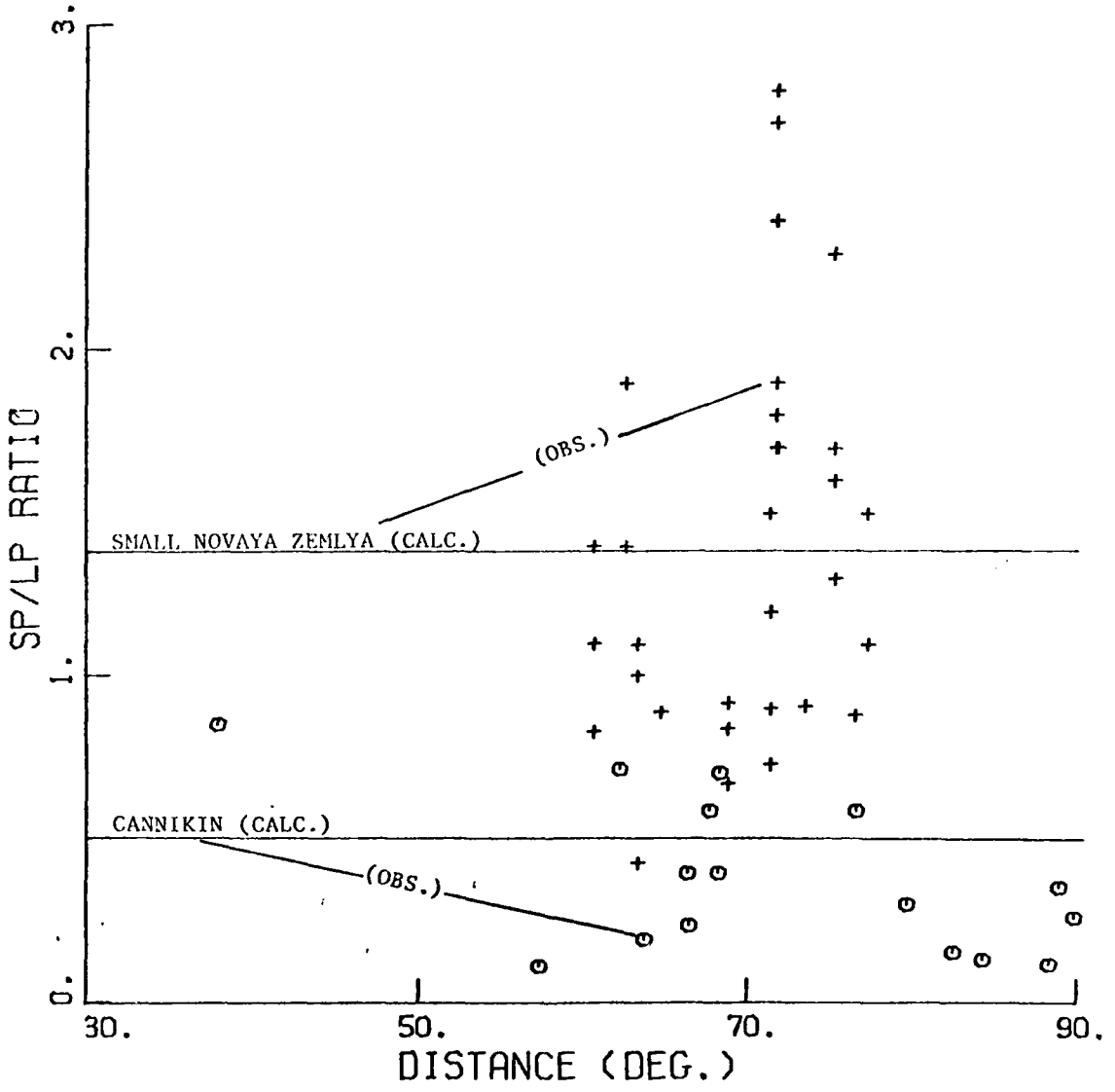
3.
2.
1.
0.
SP/LP RATIO
(OBS.)
SMALL NOVAYA ZEMLYA (CALC.)
CANNIKIN (CALC.)
(OBS.)
30.
50.
70.
90.
DISTANCE (DEG.)

Figure II-5

waveform and the amplitude ratio of the two. A much more significant conclusion is that the most important parameter in modeling the body waves is the source depth. Since the depth effect is so much more important than say the rise time or the overshoot ratio, it may be the only reliable parameter for determining yield.

III. A Comparison of Generalized Ray and Normal Mode Seismograms

David G. Harkrider and Donald V. Helmberger

The excitation of Lg_i waves is fairly well understood in the context of normal mode theory for laterally homogeneous media. Because of known lateral heterogeneities in the upper earth, and their adverse effect on Lg_i, we felt that it was important to determine the paths in the lithosphere wave guide from the source to the receiver for this energy. Once we can predict which ray paths are the major contributors to the Lg_i phases, we plan to make use of a technique for generalized rays traveling in non-uniform wave guides in order to evaluate the effect of varying the thickness of the lithospheric wave guide between source and receiver.

In order to determine the correspondence between generalized ray and normal mode theory in the generation of Lg phase we have begun a program of synthesizing seismograms for sources in simple plane layered models of the lithospheric wave guide using both generalized rays and normal modes. Here we show seismograms for a 32 km crust over a mantle half space for a horizontal pure shear dislocation source at a depth of 8 km and a surface receiver at various ranges. Figures 1 and 2 are the synthetics for the fundamental and first five overtones of the Love and Rayleigh normal modes at a range of 128 km. Figures 3 through 6 show the accumulated sum of these modes and the comparison with synthetics generated with generalized rays. This close in distance was chosen to test the significance of normal mode theory at near distances when the branch line contributions are ignored. For this particular model there are 23 Rayleigh modes and 22 Love modes in the frequency band, 0 - 2 hz, used in this example.

Since the fundamental Rayleigh wave dominates the mode sum, we show in Figures 7 and 8 the accumulated mode sum starting with the first higher mode. Using only the first six modes we demonstrate good agreement between the Rayleigh wave pulse generated by both techniques. The disagreement between the rest of the wave train is not surprising since the shear velocity of the half space is less than the compressional velocity of the upper layer and, thus, we should not have arrivals corresponding to P waves in the mode sum. The only contribution of the P waves is either diffraction phenomena or in the generation of the Rayleigh pulse.

For Love or SH waves, the agreement is good especially for the direct SH wave, i.e. the abrupt spike, and fair for the long period part of the later arrivals. Because of the long period agreement we decided to increase the source history trapezoid of $\delta t_1 = \delta t_2 = \delta t_3 = .2$ sec to .5 sec. The resulting comparison between the generalized ray and mode sum SH seismograms for ranges of 100 km to 1000 km with 100 km increments are shown in Figures 9 and 10. The agreement at all ranges is extremely good especially in the relative arrival times of various body phases in the wave train. One of the unexpected results was that the direct SH wave received most of its contribution from the Love fundamental mode at all ranges.

The individual contributions of each mode are shown in Figures 11 and 12 at ranges of 400 and 800 km. The direct SH wave appears as a large amplitude high frequency arrival preceding the fundamental airy phase. In general, the higher the mode the later its contribution to wave train. In retrospect this is not surprising, for at a given frequency in this simple model successively higher modes have higher phase velocities, i.e. smaller angles of incidence, and lower group velocities indicating that the higher

the mode the steeper the angle of incidence and the greater number of reflections and, thus, a longer travel time.

At this stage, we have not synthesized generalized rays for the P-SV system at ranges greater than 128 km. The mode sum for Rayleigh modes at a range of 1000 km is shown in Figure 13.

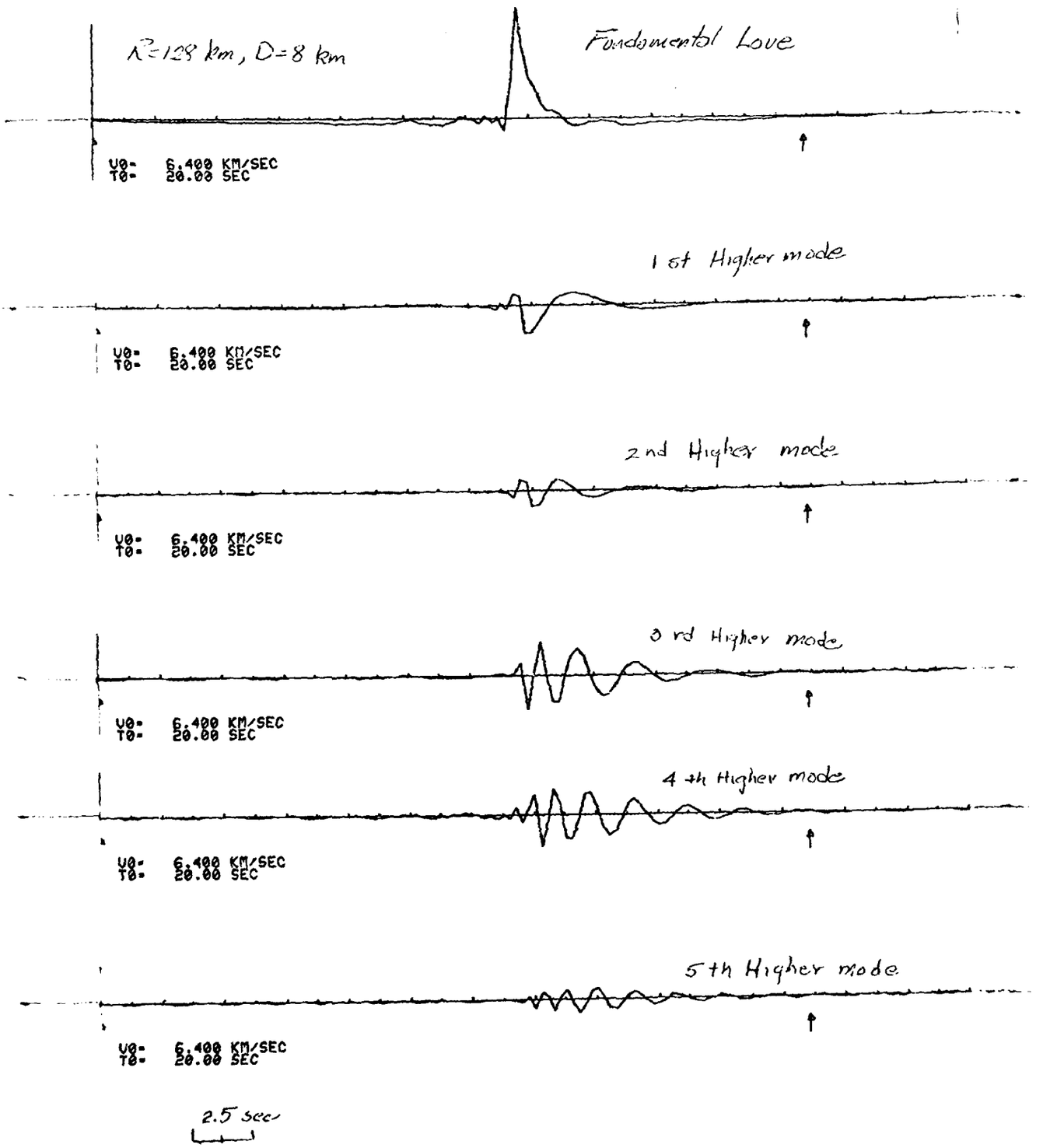
λ=128 km, D=8 km
Fundamental Love
V0= 6.400 KM/SEC
T0= 20.00 SEC
1st Higher mode
V0= 6.400 KM/SEC
T0= 20.00 SEC
2nd Higher mode
V0= 6.400 KM/SEC
T0= 20.00 SEC
3rd Higher mode
V0= 6.400 KM/SEC
T0= 20.00 SEC
4th Higher mode
V0= 6.400 KM/SEC
T0= 20.00 SEC
5th Higher mode
V0= 6.400 KM/SEC
T0= 20.00 SEC
2.5 sec

Figure III-1

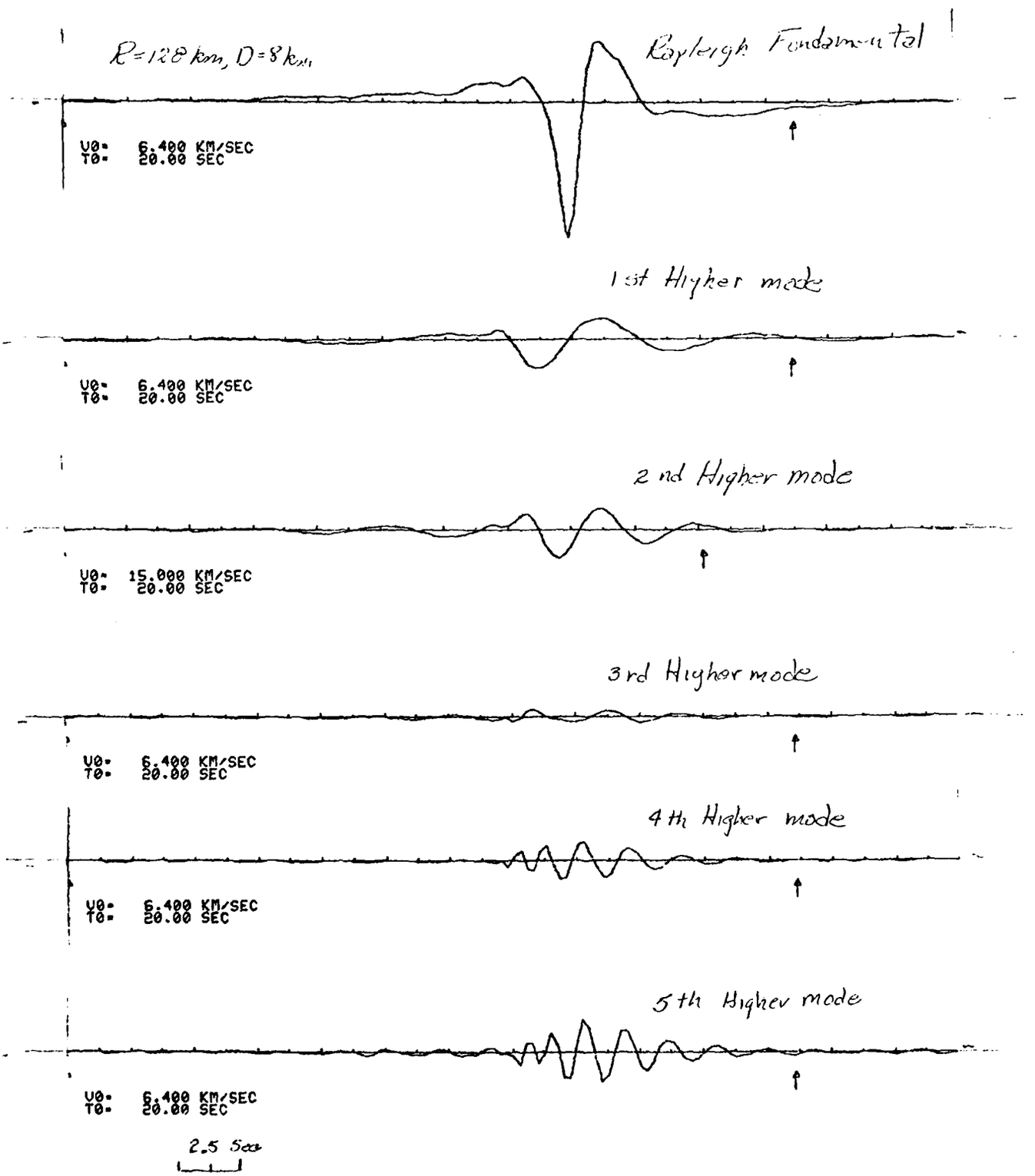
R=128 km, D=8 km
Rayleigh Fundamental
V0= 6.400 KM/SEC
T0= 20.00 SEC
1st Higher mode
V0= 6.400 KM/SEC
T0= 20.00 SEC
2nd Higher mode
V0= 15.000 KM/SEC
T0= 20.00 SEC
3rd Higher mode
V0= 6.400 KM/SEC
T0= 20.00 SEC
4th Higher mode
V0= 6.400 KM/SEC
T0= 20.00 SEC
5th Higher mode
V0= 6.400 KM/SEC
T0= 20.00 SEC
2.5 Sec

Figure III-2

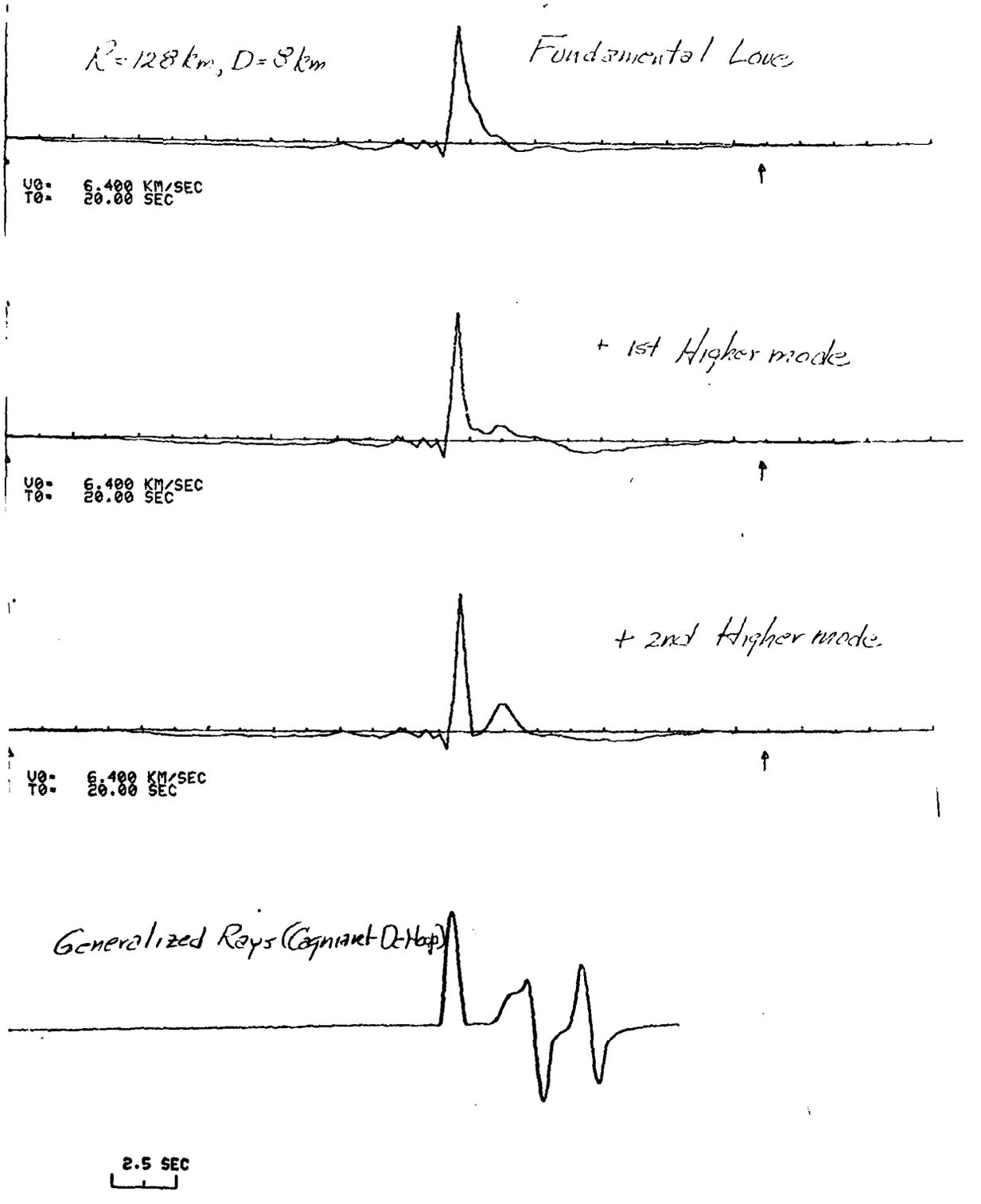
R = 128 km, D = 8 km
Fundamental Love
V0= 6.400 KM/SEC
T0= 20.00 SEC
+ 1st Higher mode
V0= 6.400 KM/SEC
T0= 20.00 SEC
+ 2nd Higher mode
V0= 6.400 KM/SEC
T0= 20.00 SEC
Generalized Rays (Cagniard-De Hoop)
2.5 SEC

Figure III-3

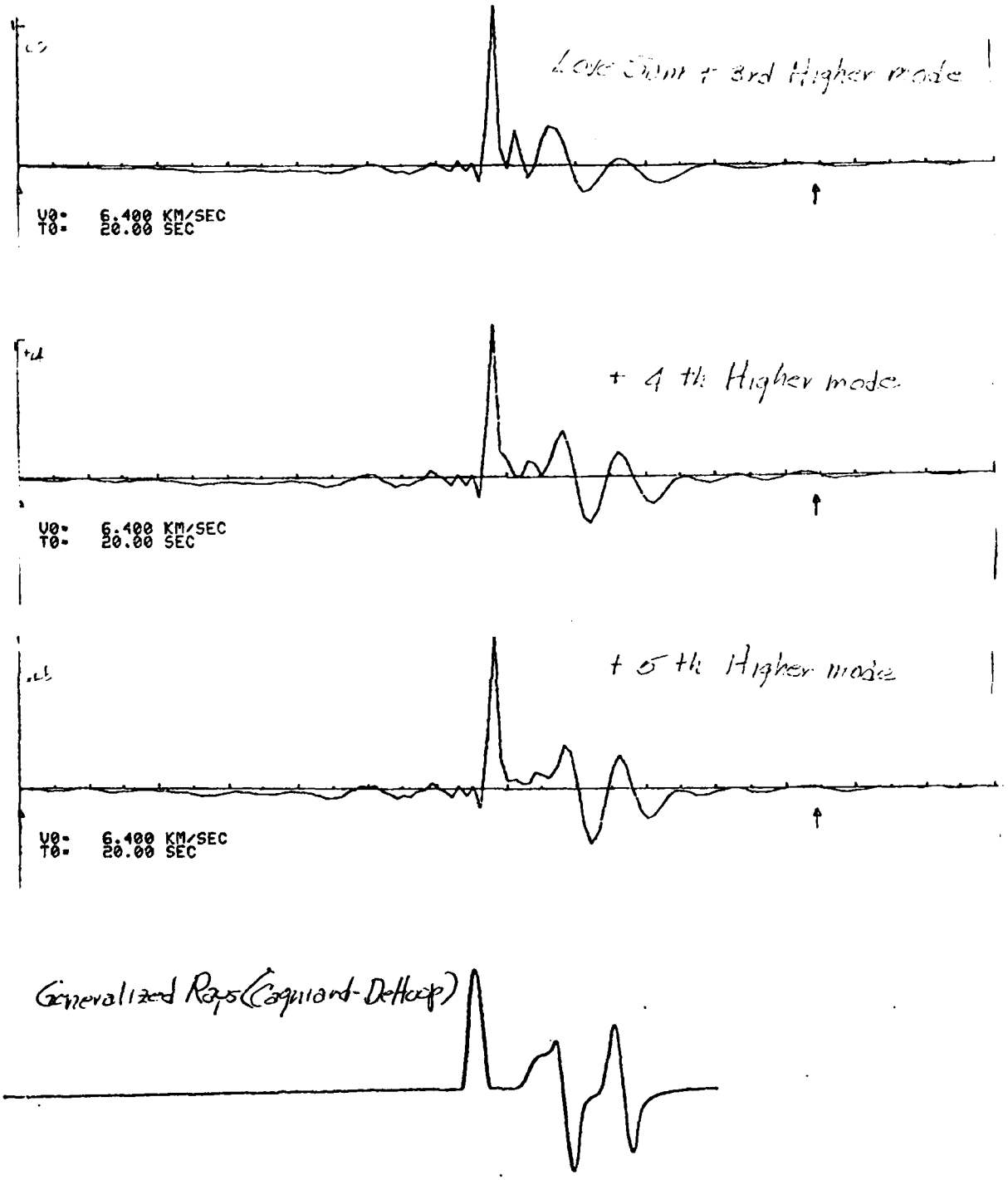
Love 3rd + 3rd Higher mode
V0= 6.400 KM/SEC
T0= 20.00 SEC
+ 4 th Higher mode
V0= 6.400 KM/SEC
T0= 20.00 SEC
+ 5 th Higher mode
V0= 6.400 KM/SEC
T0= 20.00 SEC
Generalized Rays (Cagniard-DeHoop)
2.5 SEC

Figure III-4

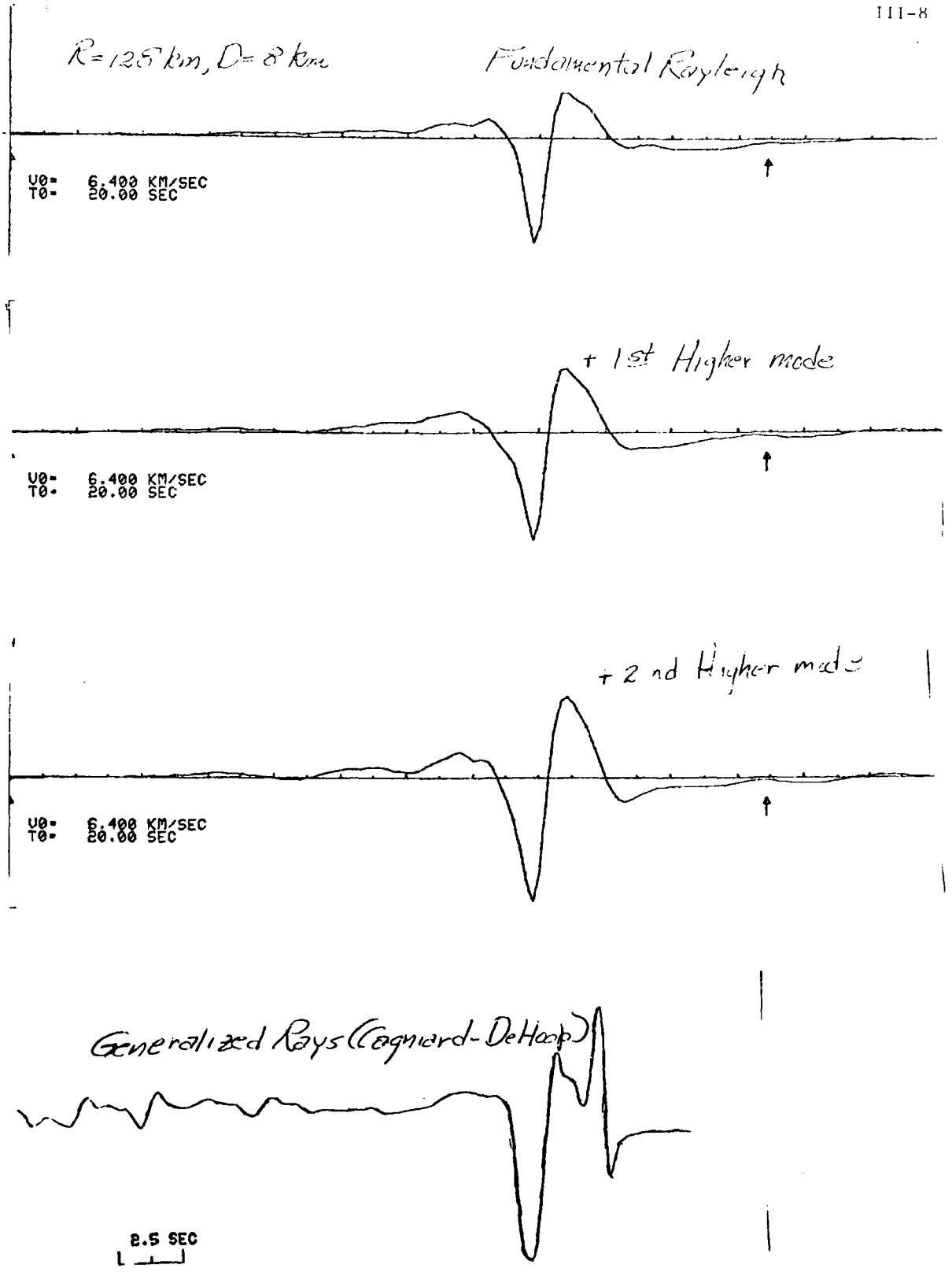
R = 125 km, D = 8 km
Fundamental Rayleigh
U0= 6.400 KM/SEC
T0= 20.00 SEC
+ 1st Higher mode
U0= 6.400 KM/SEC
T0= 20.00 SEC
+ 2nd Higher mode
U0= 6.400 KM/SEC
T0= 20.00 SEC
Generalized Rays (Cagniard-DeHoop)
2.5 SEC

Figure III-5

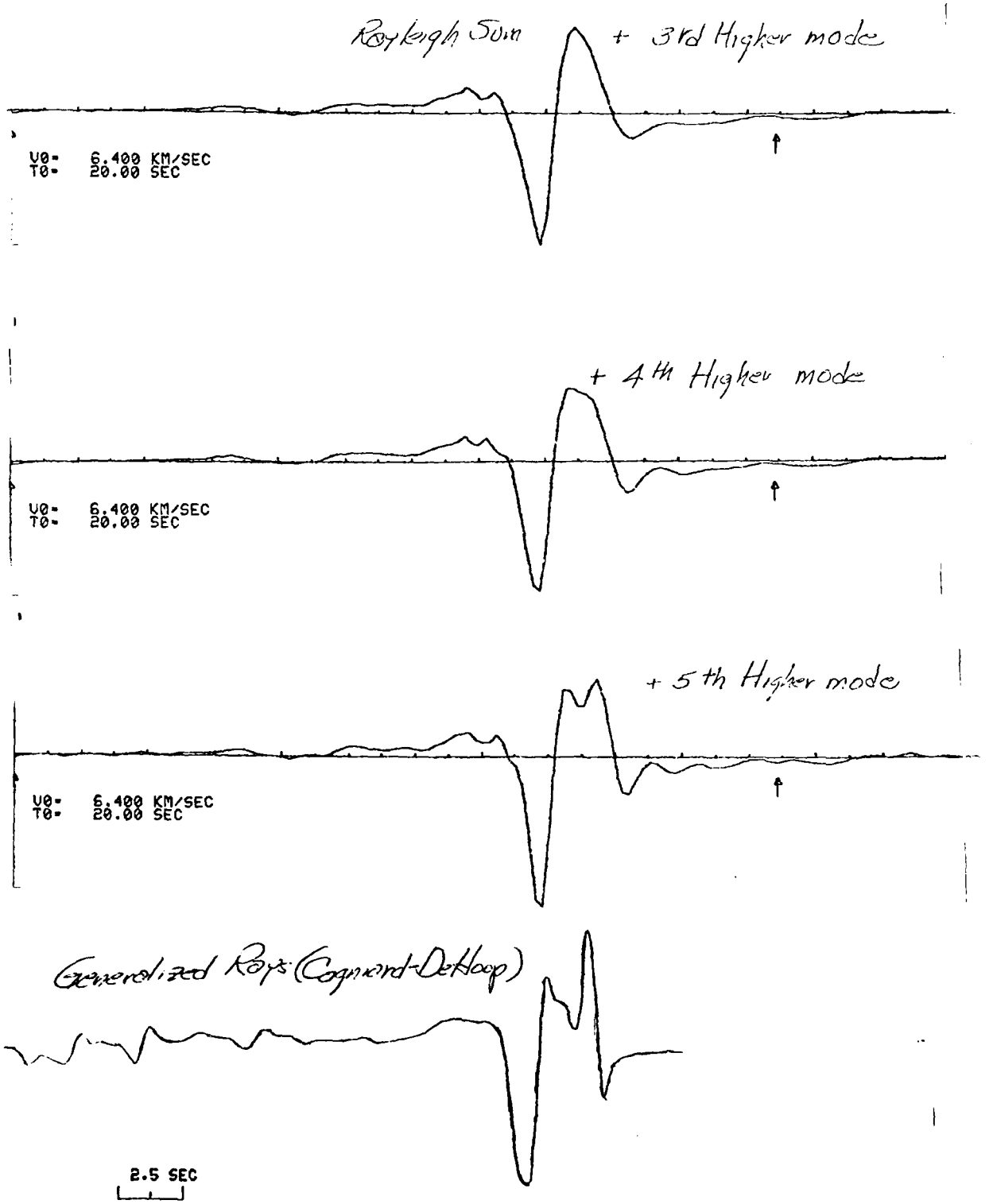
Rayleigh Sum
+ 3rd Higher mode
V0= 6.400 KM/SEC
T0= 20.00 SEC
+ 4th Higher mode
V0= 6.400 KM/SEC
T0= 20.00 SEC
+ 5th Higher mode
V0= 6.400 KM/SEC
T0= 20.00 SEC
Generalized Rays (Cagniard-DeHoop)
2.5 SEC

Figure III-6

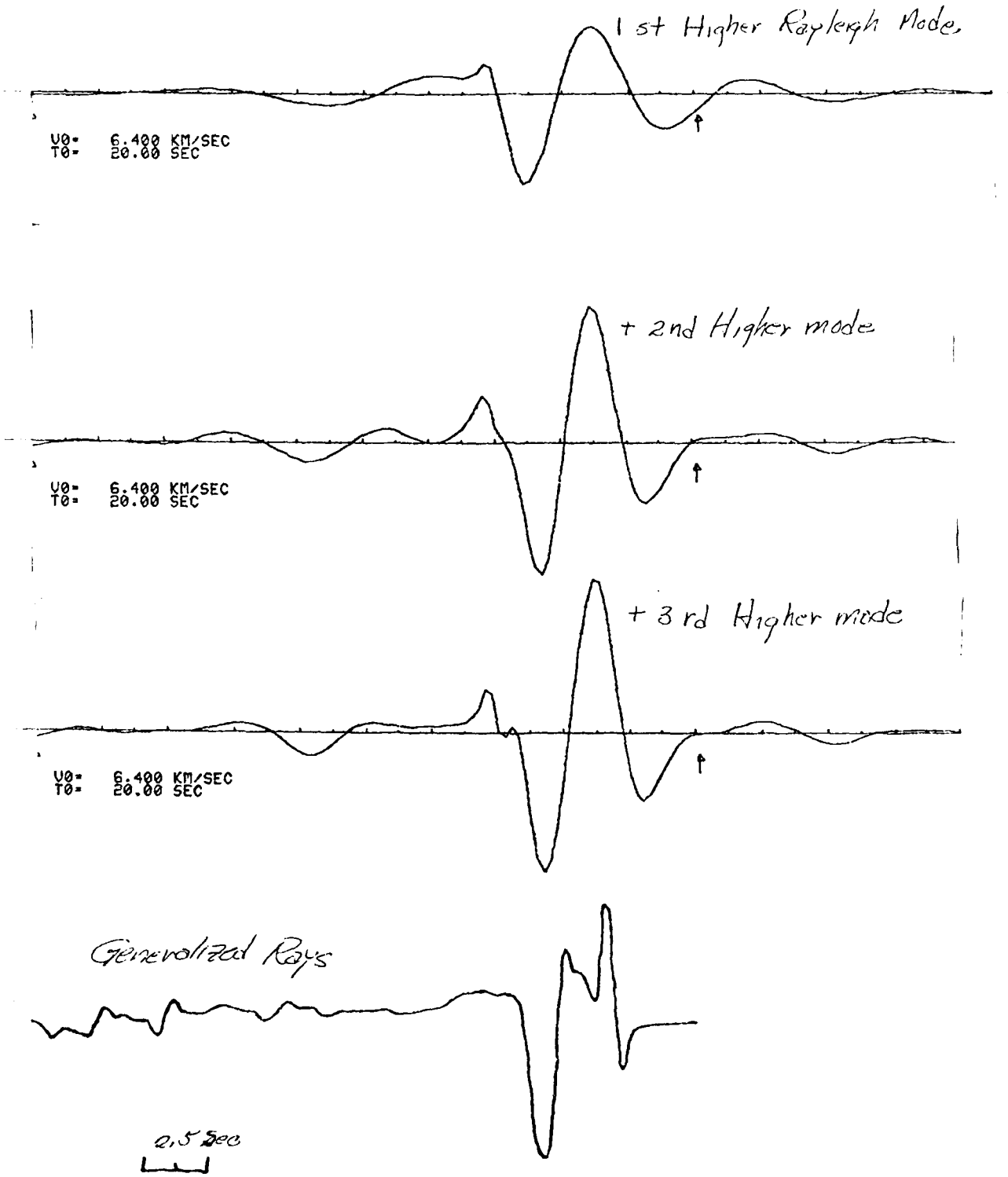
1 st Higher Rayleigh Mode
V0= 6.400 KM/SEC
T0= 20.00 SEC
+ 2nd Higher mode
V0= 6.400 KM/SEC
T0= 20.00 SEC
+ 3 rd Higher mode
V0= 6.400 KM/SEC
T0= 20.00 SEC
Generalized Rays
0.5 Sec

Figure III-7

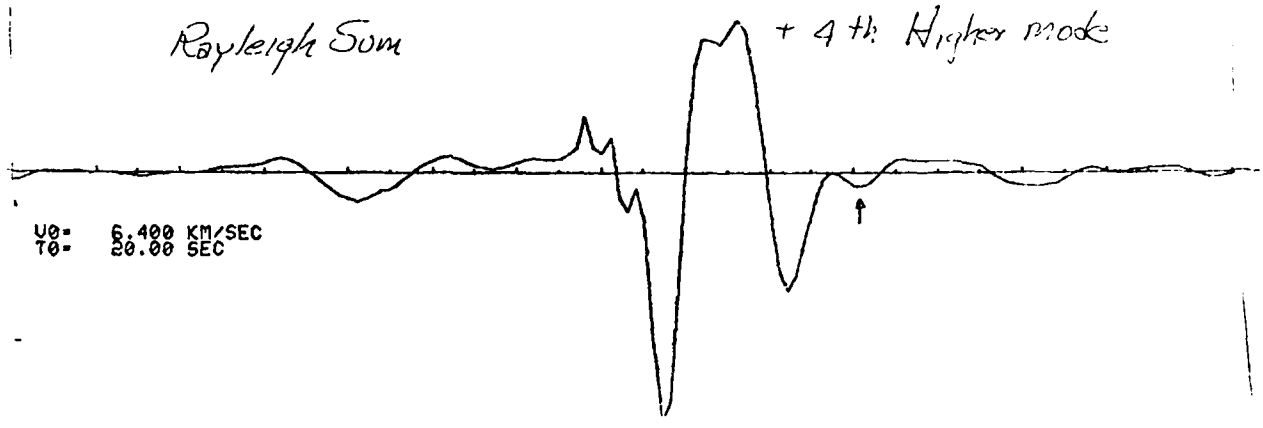

UT

2.5 sec

U

Figure III-8

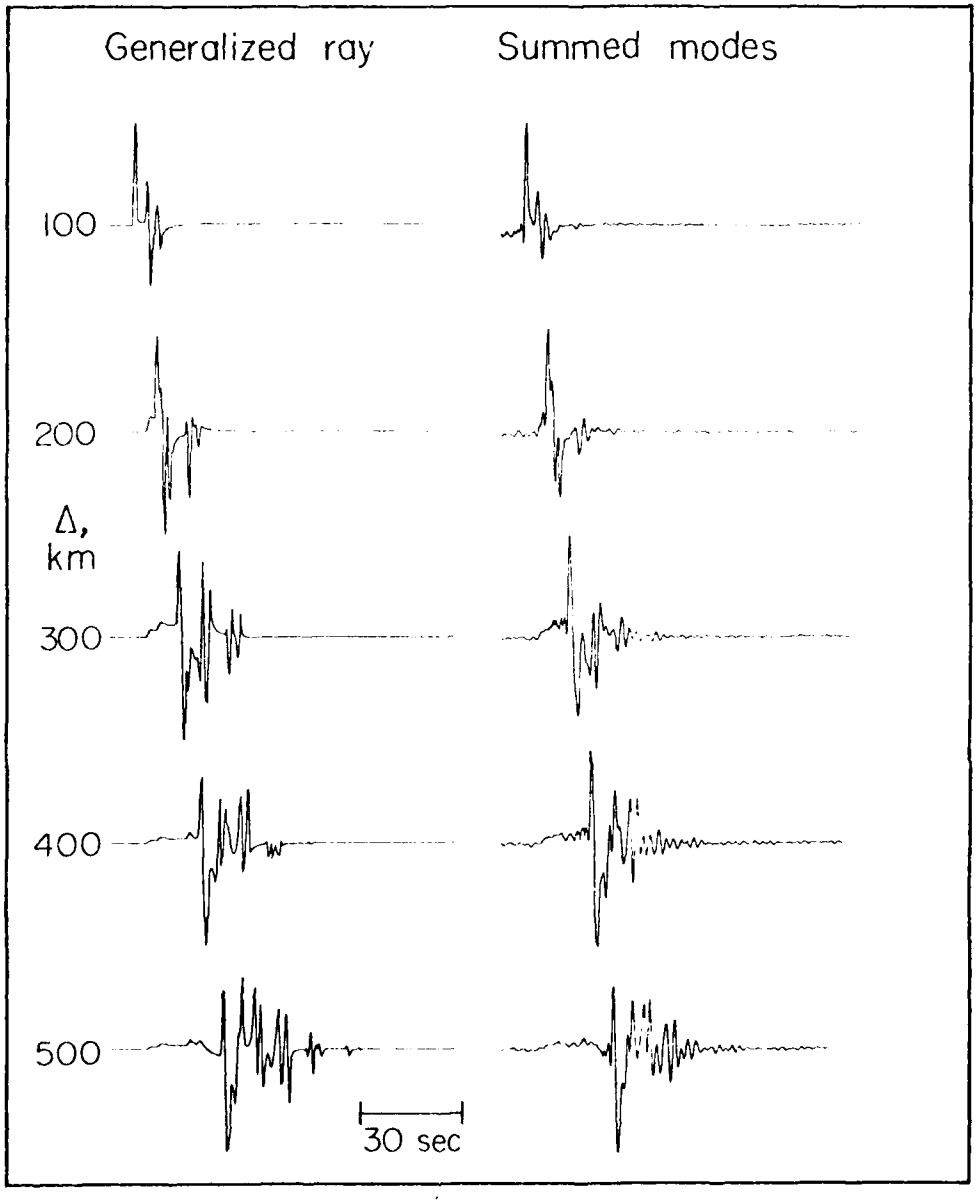

Figure 9

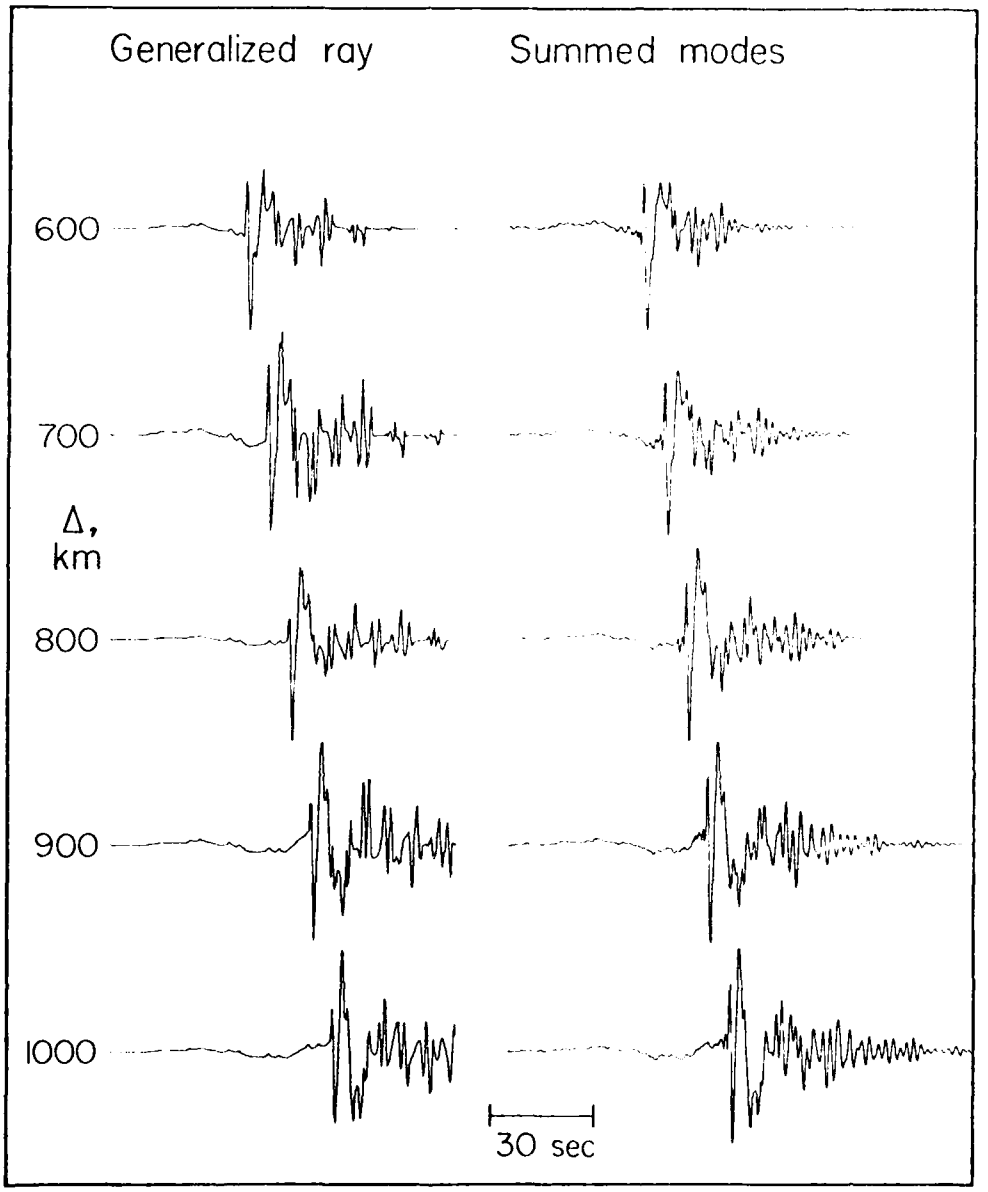

Figure 10

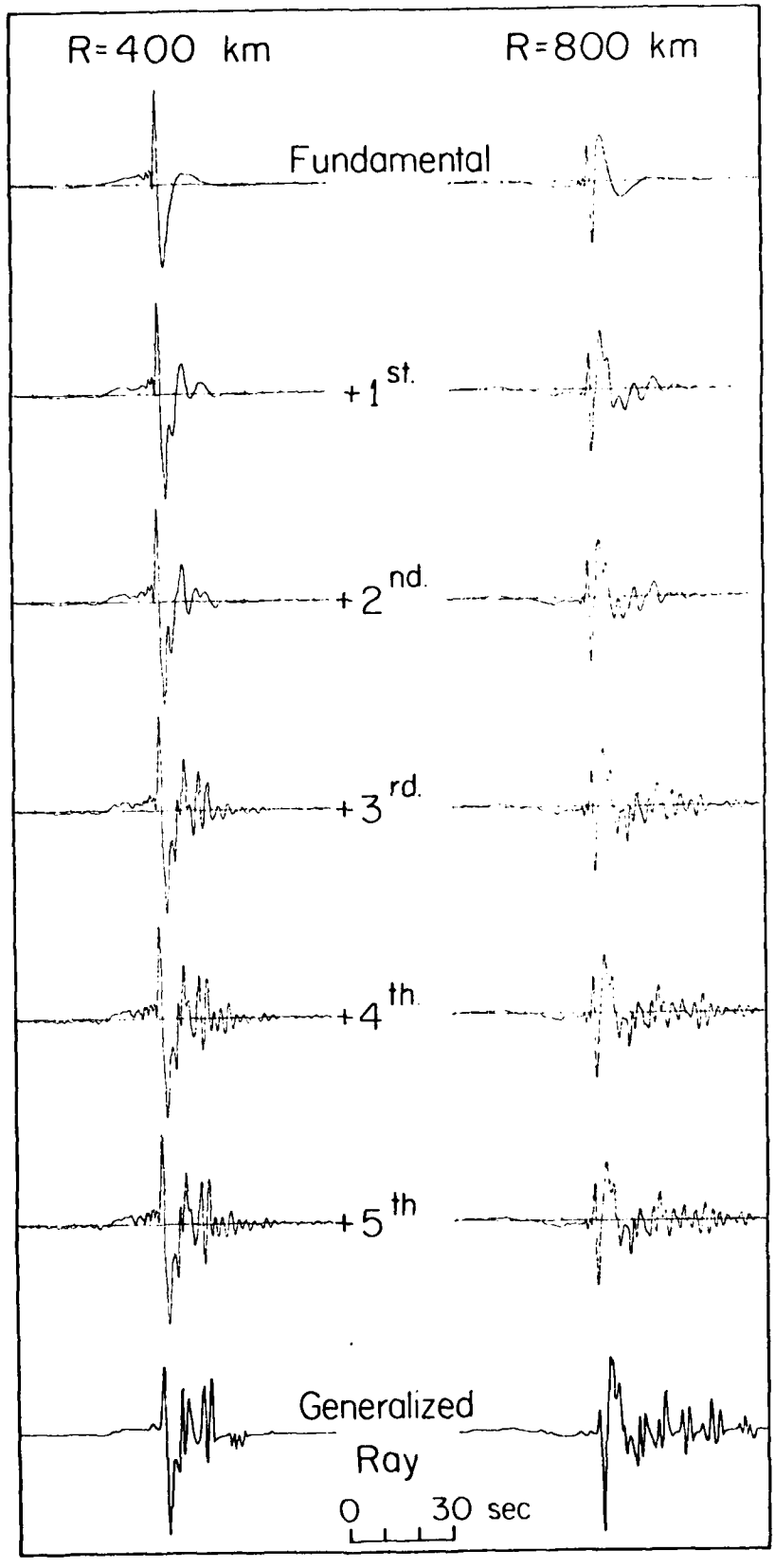

Figure 11

Figure 12

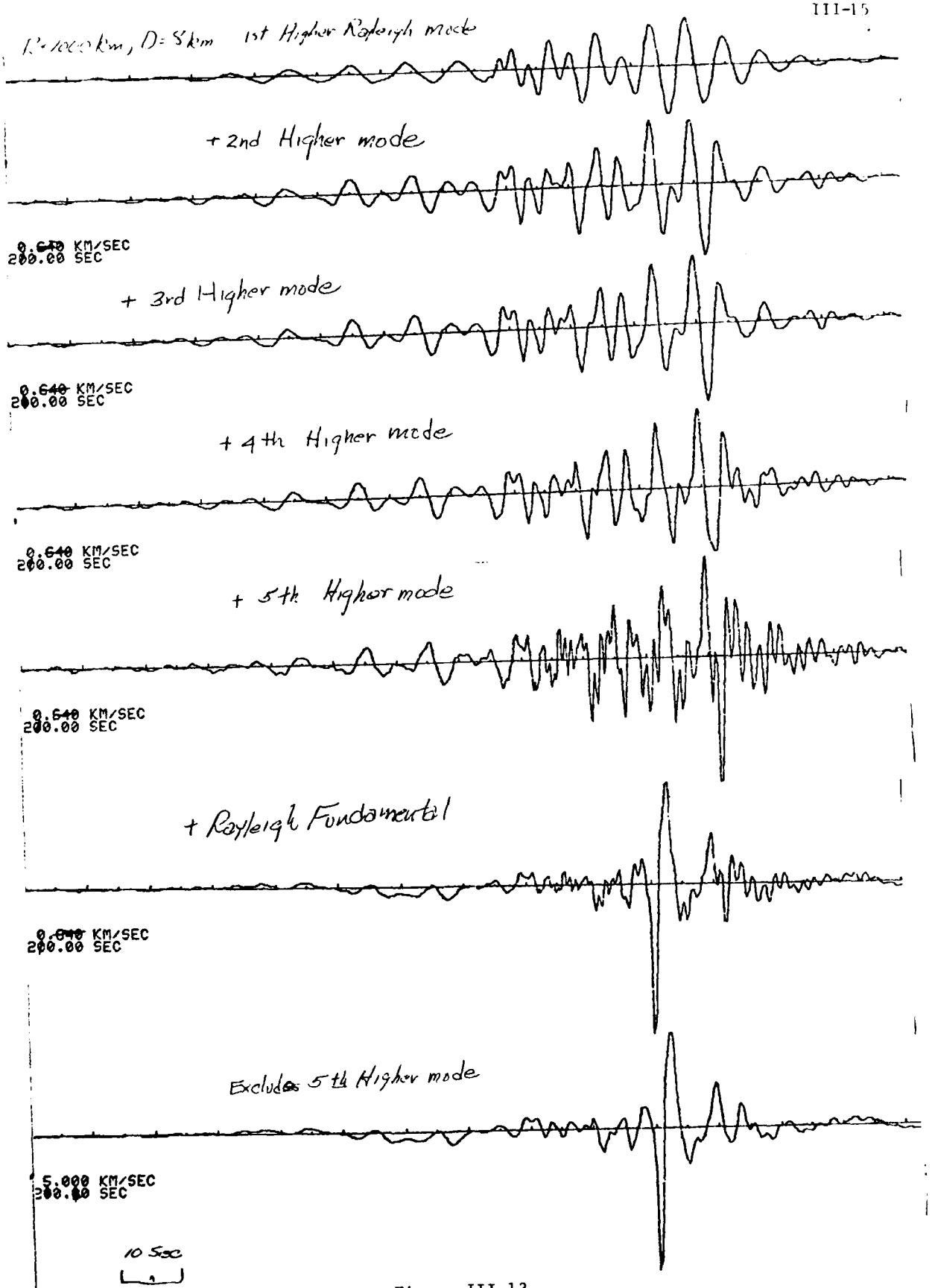

Figure III-13

IV. Modeling Earthquakes with Generalized Ray Theory*

Donald V. Helmberger

and

David G. Harkrider

Abstract

The complete linear response of plane, elastic layered solid to a shear dislocation is investigated. The solution is expressed as a summation of generalized rays of the P, SV, and SH potentials. This allows the transient response to be obtained upon application of the Cagniard-de Hoop technique. Numerical results of the full solution containing the near and far field terms are compared for a whole space, half space, and layered model with asymptotic solutions to establish the advantages and limitations of approximate methods.

*Contribution No. 2959, Division of Geological and Planetary Sciences, California Institute of Technology, Pasadena, CA 91125

Introduction

In the past decade, significant progress in our understanding of seismograms has been accomplished based largely on our ability to separate source effects from propagational distortions. Numerous formalisms have been developed whereby synthetic seismograms can be computed at various positions on the Earth, for comparisons with observed seismograms. Iterative techniques can then be applied to determine Earth structure or source models or perhaps some properties of both. The most efficient technique used to generate synthetics is essentially controlled by the ratio of the travel time of the disturbance to the source duration, with optics at the upper limit and statics at the lower. However, a highly desirable property of any technique is that the physics be relatively apparent so that the user can easily discern how model parameters influence the synthetic motion. In this paper we will discuss such a technique, called generalized ray theory, where various useful approximations are made based on the travel time to duration ratio.

We assume that earthquakes can be simulated by distributed shear dislocations and that the Earth can be replaced by a layered elastic medium; both assumptions are suspect but worth consideration as viable models at our present level of understanding.

First, we will consider a shear dislocation in a whole space expressed in cylindrical coordinates becasue of its compatibility with the layered problem. The layered structure complication is effectively removed by a generalized ray expansion of the P, SV, and SH displacement potentials with the Cagniard-de Hoop technique used to obtain the transient response.

This basic technique has been used earlier by Pekeris (1940) and his colleagues and is sometimes called the Cagniard-Pekeris method by Ben-Menahem and Vered (1973). Japanese seismologists use a similar technique and call it the Cagniard-de Hoop-Sato method (Kawasaki et al., 1973). The basic idea appears to have originated with Lamb (1904) and has been modified for special purposes by many researchers.

Shear Dislocation Source

Haskell (1964) introduced a shear fault where a discontinuity in displacement across a fault plane was allowed resulting in a double-couple radiation pattern. Following De Hoop's (1958) form of the elastodynamic representation Harkrider (1976) has obtained convenient forms of displacements and displacement potentials for a number of different coordinate systems. The solution in cylindrical coordinates has been further reduced to a form suitable for the application of Cagniard's method by Helmberger (1974), and Langston and Helmberger (1975). The results in terms of the Laplaced transformed displacements along the vertical, tangential, and radial directions are:

$$\hat{W} = \frac{\partial \hat{\phi}}{\partial z} + sp\hat{\Omega}$$

$$\hat{V} = \frac{1}{r}\frac{\partial \hat{\phi}}{\partial \theta} - \frac{1}{spr}\frac{\partial^2 \hat{\Omega}}{\partial z \partial \theta} - \frac{\partial \hat{\chi}}{\partial r} \qquad (1)$$

$$\hat{Q} = \frac{\partial \hat{\phi}}{\partial r} - \frac{1}{sp}\frac{\partial^2 \hat{\Omega}}{\partial r \partial z} + \frac{1}{r}\frac{\partial \hat{\chi}}{\partial \theta}$$

where z, r, and 0 are the vertical, radial, and polar angle coordinates respectively. The P wave potential (ϕ), the SV wave potential (Ω), and the SH wave potential (χ) are expressed by:

P-wave:

$$\hat{\phi} = + \frac{M_o}{4\pi\rho} \frac{2}{\pi} Im \int_c^{+i\infty+c} C_1(p) \frac{p}{\eta_\alpha} \exp(-s\eta_\alpha|z-h|)K_2(spr)dp.A_1(\theta,\lambda,\delta)$$

$$+ \frac{M_o}{4\pi\rho} \frac{2}{\pi} Im \int_c^{+i\infty+c} C_2(p) \frac{p}{\eta_\alpha} \exp(-s\eta_\alpha|z-h|)K_1(spr)dp.A_2(\theta,\lambda,\delta)$$

$$+ \frac{M_o}{4\pi\rho} \frac{2}{\pi} Im \int_c^{+i\infty+c} +C_3(p) \frac{p}{\eta_\alpha} \exp(-s\eta_\alpha|z-h|)K_o(spr)dp.A_3(\theta,\lambda,\delta). \quad (2)$$

SV-waves:

$$\hat{\Omega} = + \frac{M_o}{4\pi\rho} \frac{2}{\pi} Im \int_c^{+i\infty+c} SV_1(p) \frac{p}{\eta_\beta} \exp(-s\eta_\beta|z-h|)K_2(spr)dp.A_1(\theta,\lambda,\delta)$$

$$+ \frac{M_o}{4\pi\rho} \frac{2}{\pi} Im \int_c^{+i\infty+c} SV_2(p) \frac{p}{\eta_\beta} \exp(-s\eta_\beta|z-h|)K_1(spr)dp.A_2$$

$$+ \frac{M_o}{4\pi\rho} \frac{2}{\pi} Im \int_c^{+i\infty+c} SV_3(p) \frac{p}{\eta_\beta} \exp(-s\eta_\beta|z-h|)K_o(spr)dp.A_3 .$$

SH-waves:

$$\hat{\chi} = + \frac{M_o}{4\pi\rho} \frac{2}{\pi} Im \int_c^{+i\infty+c} SH_1(p) \frac{p}{\eta_\beta} \exp(-s\eta_\beta|z-h|)K_2spr)dp.A_4$$

$$+ \frac{M_o}{4\pi\rho} \frac{2}{\pi} Im \int_c^{+i\infty+c} SH_2(p) \frac{p}{\eta_\beta} \exp(-s\eta_\beta|z-h|)K_1(spr)dp.A_5$$

where only the first term of each potential is required in describing a pure strike-slip and the second term only for a pure dip-slip orientation (Harkrider, 1976). The more important definitions are as follows:

s = Laplace transform variable

p = ray parameter

$\eta_v = \left(\frac{1}{V^2} - p^2\right)^{\frac{1}{2}}$

h = depth of source

α = compressional velocity

β = shear velocity

ρ = density

M_o = seismic moment

with the orientation constants given by:

$$A_1(\theta,\lambda,\delta) = \sin 2\theta \cos\lambda \sin\delta + \frac{1}{2}\cos 2\theta \sin\lambda \sin 2\delta$$

$$A_2(\theta,\lambda,\delta) = \cos\theta \cos\lambda \cos\delta - \sin\theta \sin\lambda \cos 2\delta \qquad (3)$$

$$A_3(\theta,\lambda,\delta) = \frac{1}{2}\sin\lambda \sin 2\delta$$

$$A_4(\theta,\lambda,\delta) = \cos 2\theta \cos\lambda \sin\delta - \frac{1}{2}\sin 2\theta \sin\lambda \sin 2\delta$$

$$A_5(\theta,\lambda,\delta) = -\sin\theta \cos\lambda \cos\delta - \cos\theta \sin\lambda \cos 2\delta$$

where

θ = strike from the end of the fault plane

λ = rake angle

δ = dip angle

The vertical radiation patterns, as will become apparent shortly, are defined by

$$C_1 = -p^2 \qquad SV_1 = -\varepsilon p \eta_\beta \qquad SH_1 = \frac{1}{\beta^2}$$

$$C_2 = 2\varepsilon p \eta_\alpha \qquad SV_2 = (\eta_\beta^2 - p^2) \qquad SH_2 = -\frac{\varepsilon}{\beta^2}\frac{\eta_\beta}{p} \tag{4}$$

$$C_3 = (p^2 - 2\eta_\alpha^2) \qquad SV_3 = 3\varepsilon p \eta_\beta$$

where $\varepsilon = \begin{cases} +1 & z > h \\ -1 & z < h \end{cases}$

The integrals expressed in (2) can be transformed back into the time domain by the application of the Cagniard-de Hoop technique, see Gilbert and Helmberger (1972) and Harkrider and Helmberger (1977). For example, the field function defined by

$$\bar{\zeta}_n(r,z,s) = \frac{2}{\pi} s \;\; Im \int_c^{i\infty+c} \frac{p}{\eta_v} K_n(spr)\, e^{-s\eta_v|z-h|} dp \tag{5}$$

becomes

$$\zeta_n(r,z,t) = \frac{2}{\pi}\frac{\partial}{\partial t} \;\; Im \int_o^t \frac{c_n(t,\tau)}{(t-\tau)^{1/2}\,(t-\tau+2pr)^{1/2}} \left(\frac{dp}{d\tau}\right) \frac{p(\iota)}{\eta_v} \, d\tau \;, \tag{6}$$

where

$$c_n(t,\tau(p)) = \cosh\left(n \cosh^{-1}\left(\frac{t-\tau+pr}{pr}\right)\right)$$

The geometry is given in Figure 1a and the de Hoop contour Γ in Figure 1b, see de Hoop (1960). The various functions of p are to be evaluated along Γ defined by choosing those values of p which make $\tau(p)$ real and increasing where

$$\tau(p) = pr + \eta_v |z-h| \quad . \tag{7}$$

Thus,

$$p(\tau) = \frac{r}{R^2}\tau + i\left(\tau^2 - \frac{R^2}{V^2}\right)^{1/2} |z-h| \tag{8}$$

and

$$\eta(\tau) = \frac{|z-h|\tau}{R^2} - i\left(\tau^2 - \frac{R^2}{V^2}\right)^{1/2} \frac{r}{R^2} \tag{9}$$

and

$$\frac{dp(\tau)}{d\tau} = \frac{i\,\eta_v(\tau)}{(-R^2/V^2)^{1/2}} \tag{10}$$

where

$$R^2 = r^2 + |z-h|^2$$

Note that the integrand is real until

$$p = p_o = \frac{r}{RV} = \frac{\sin i}{V}$$

which is the ray parameter corresponding to Snell's law.

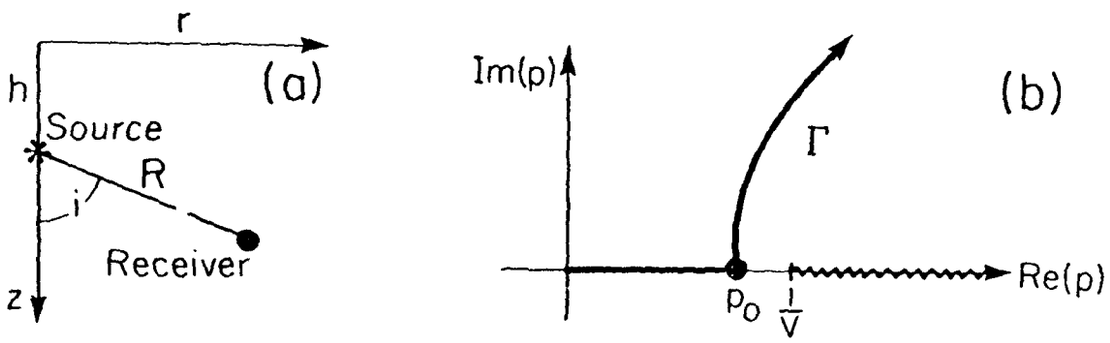

Figure IV-1. Source-receiver geometry and complex (p) plane with branch cut starting at (1/V) and running out along the real (p) axes.

In this simple case we have a closed form solution for various values of n since the equivalent form back in the (ω,k) domain has been evaluated by Harkrider (1976). For example,

$$\zeta_2(r,z,t) = \frac{\partial}{\partial t}\left\{\left[\frac{1}{R} + \frac{2V}{r^2}\left(t - \frac{R}{V}\right)\right] H\left(t - \frac{R}{V}\right)\right\} \tag{11}$$

where the near-field contribution appears in terms of r. However, since we need to evaluate integrals similar to (2) with complicated complex integrands later it should be noted that (6) can be evaluated for various values of (t) after a change of variable as proposed by Helmberger (1968). A relatively fast evaluation of this type of integral is by nonuniform quadrature techniques where the point spacing is determined by the rate of change of the integrand. The accuracy of such techniques will be

discussed later. First we will examine some useful approximations by expanding the integrand of (6) in terms of $(t-\tau)^{-1/2}$. Note that

$$c_n(t,\tau,p) = \frac{1}{2}\left[\frac{(y+(y^2-1)^{1/2})^{2n}+1}{(y+(y^2-1)^{1/2})^{n}}\right]$$

where

$$y = \frac{t-\tau+pr}{pr}$$

and

$$\frac{c_n(t,\tau,p)}{(t-\tau+2pr)^{1/2}} \approx \frac{1}{\sqrt{2pr}}$$

to first order. Thus, we can approximate (6) by

$$\zeta_n(v,z,t) = \frac{2}{\pi}\frac{\partial}{\partial t} Im \int_o^t \frac{1}{\sqrt{2pr}} \frac{1}{(t-\tau)^{1/2}} \frac{dp}{dt}\frac{p}{\eta_v}\, d\tau \qquad (12)$$

$$= \frac{d}{dt}\left[\frac{1}{\sqrt{t}} * Im\left(\sqrt{\frac{2}{r}}\frac{1}{\pi}\frac{\sqrt{p}}{\eta_v}\frac{dp}{dt}\right)\right]$$

when treating a high frequency source with duration, T, such that $T << 2pr$.

A still further approximation can be used at very large r's when

$$\frac{dp}{dt} = i\,(t-t_R)^{-1/2}\,\frac{\eta_v}{(2t_R)^{1/2}}$$

where $t_R = R/V$ and $p = p_o$ and (12) reduces to

$$\zeta_n(r,z,t) = \frac{\delta(t-t_R)}{R} \tag{13}$$

called the first motion approximation. This approximation is valid at teleseismic distances where the ratio of travel time to duration is of the order of 100 or greater and has proven quite useful in modeling shallow earthquakes, see Langston and Helmberger (1975).

The approximation used in (12) can be obtained in a slightly simpler way by returning to expression (5) and using the asymptotic form of the modified Bessel function, namely

$$K_n(spr) = \sqrt{\frac{\pi}{2spr}}\ e^{-spr}\left[1 + \frac{\mu-1}{8spr} + \ldots\right]$$

where $\mu = 4n^2$. Substitution of the first term of the above expression into (5) yields (12) after applying the de Hoop (1960) technique. Note that the second order term has the form of a temporal integration of the first term or the form of a near-field effect. We will discuss the high frequency solution in the next section keeping only the first term; however, the further expansion in higher order terms can be carried out in similar fashion and will be discussed in the numerical results.

High Frequency Solution for a Multi-Layer Problem

Applying the method of generalized reflection and transmission coefficients (Spencer, 1960), it is possible to construct a representation for

a disturbance which has traversed some layering in some specified mode of propagation. The tangential displacement on the surface of a layered half-space model where only the far-field term is retained becomes

$$V(r,o,\theta,t) = \frac{M_o}{4\pi\rho_o}\frac{d}{dt}\left[\dot{D}(t)*\sum_{j=1}^{2}A_{j+3}(\theta,\lambda,\delta)V_j(t)\right] \tag{14}$$

where

$$V_j(t) = \frac{2}{r}\frac{1}{\pi}\frac{1}{\sqrt{t}} * Im\left[\left(\sum_{i=1}^{n}\frac{\sqrt{p}}{\eta_\beta}SH_j(p)\Pi(p)(p)\frac{dp}{dt}\right)_i\right]$$

$\dot{D}(t)$ = far field time history

$\Pi_i(p)$ = product of reflection and transmission coefficients and the summation is over contributing rays. Numerical evaluation of these expressions are discussed in detail by Helmberger and Malone (1975).

The high frequency approximations for the other components of motion are somewhat more complicated with the vertical displacement on the free surface given by

$$W(r,o,\theta,t) = \frac{M_o}{4\pi\rho_o}\frac{d}{dt}\left[\dot{D}(t)*\sum_{j=1}^{3}A_jW_j\right] \tag{15}$$

where

$$W_j(t) = \sqrt{\frac{2}{r}}\frac{1}{\pi}\left[\frac{1}{\sqrt{t}} * \sum_{i=1}^{n} Im\left(\frac{\sqrt{p}}{\eta_\alpha} C_j(p) R_{NZ}(p) \Pi_i(p) \frac{dp}{dt}\right)_i\right]$$
$$+\sqrt{\frac{2}{r}}\frac{1}{\pi}\left[\frac{1}{\sqrt{t}} * \sum_{i=1}^{n} Im\left(\frac{\sqrt{p}}{\eta_\beta} SV_j(p) R_{NZ}(p) \Pi_i(p) \frac{dp}{dt}\right)_i\right]$$

The function $\Pi_i(p)$ defines the product of all transmission and reflection coefficients along the path from the source to the receiver. The function $R_{NZ}(p)$ is defined by $R_{PZ}(p)$ or $R_{SZ}(p)$ depending on the mode of propagation upon arrival at the receiver,

with

$$R_{PZ} \equiv \frac{2\eta_\alpha(\eta_\beta^2 - p^2)}{\beta^2 R(p)}$$

$$R_{SZ} \equiv \frac{4p\eta_\alpha\eta_\beta}{\beta^2 R(p)} \qquad (16)$$

$$R(p) \equiv (\eta_\beta^2 - p^2)^2 + 4p^2\eta_\alpha\eta_\beta \qquad (17)$$

R_{PZ} and R_{SZ} are called receiver functions and are derived by taking the limiting conditions as direct P, reflected PP, and SP converge in time at a free surface, see Knopoff et al. (1957) and Helmberger (1974).

The radial displacement, Q, is obtained by replacing R_{PZ} and R_{SZ} by R_{PR} and R_{SR} defined by

$$R_{PR} = \frac{-4\eta_\alpha \eta_\beta p}{\beta^2 R(p)}$$

$$R_{SR} = \frac{2\eta_\beta (\eta_\beta^2 - p^2)}{\beta^2 R(p)} \qquad (18)$$

The reflection and transmission coefficients used in $\Pi_i(p)$ are those defined by Helmberger (1968). Synthetic responses for these solutions will be discussed after we examine the full Cagniard solution.

Full Cagniard Solution

The high frequency solution discussed in the last section has many advantages in model studies due to its simplicity. However, for small values of (spr), one must use the full solution by applying the transformations used in deriving expression (6). The displacements given by (1) can be evaluated by substituting the potentials (2) and inverting the various terms back into the time domain. The vertical displacement becomes

$$W(r,z,\theta,t) = \frac{M_o}{4\pi\rho_o} \frac{d}{\partial t} \left[\dot{D}(t) * \sum A_j W_j \right] \tag{19}$$

where W_1, W_2, and W_3 correspond to a pure strike-slip, dip-slip, and 45° dip-slip respectively. The strike-slip response can be written

$$W_1(r,z,\theta,t) = \frac{2}{\pi} Im \int^t g_\alpha(2) C_1 R_{PZ} dt + \frac{2}{\pi} Im \int^t g_\beta(2) SV_1 R_{SZ} dt \tag{20}$$

where

$$g_v(n) = C(t,\tau,n) \frac{p}{\eta_v} \left(\frac{dp}{dt}\right) (t-\tau+2p\tau)^{-1/2} (t-\tau)^{-1/2}$$

and

$$R_{PZ} = \eta_\alpha \ , \ R_{SZ} = p \text{ for a whole space.}$$

They are given by expression (16) for a receiver on the free surface. Similar expressions are obtained for the dip-slip and 45° dip-slip cases with n = 1 and n = 0 respectively.

The tangential displacement is slightly more complicated because of the explicit near-field terms

$$V(r,z,\theta,t) = \frac{M_o}{4\pi\rho_o} \frac{d}{dt} \left[\dot{D}(t) * \sum_{j=1}^{2} A_{j+3} V_j \right] \tag{21}$$

$$V_1(r,z,\theta,t) = \frac{2}{\pi} Im \int^t g_\beta(1) SH_1 R_T d\tau$$

$$+ \frac{2}{\pi} Im \iint^t g_\beta(2) SH_1 R_T \left(\frac{2}{pr}\right) d\tau dt$$

$$+ \frac{2}{\pi} Im \iint^t g_\alpha(2) C_1 R_{PT} \left(\frac{2}{r}\right) d\tau dt \qquad (22)$$

$$+ \frac{2}{\pi} Im \iint^t g_\beta(2) SV_1 R_{ST} \left(\frac{2}{r}\right) d\tau dt$$

where

$$R_T = p, \; R_{PT} = 1, \; R_{ST} = -\eta_\beta/p \text{ for whole space}$$

and

$$R_T = 2p$$

$$R_{PT} = \frac{4\eta_\alpha \eta_\beta}{\beta^2 R(p)}$$

$$R_{ST} = \frac{-2\eta_\beta}{p} \frac{(\eta_\beta^2 - p^2)}{\beta^2 R(p)}$$

for a receiver on the free surface. The dip-slip result is similar with n = 1 and where the factor in parentheses is reduced by two.

Finally, the most complicated radial component is expressed by

$$Q(r,z,\theta,t) = \frac{M_o}{4\pi\rho_o} \frac{d}{dt} \left[\dot{D}(t) * \sum_{j=1}^{3} A_j Q_j \right] \qquad (23)$$

where

$$Q_1(r,z,\theta,t) = \frac{2}{\pi}\int^{t} g_\alpha(1)C_1R_{PR}d\tau + \frac{2}{\pi}\int^{t} g_\beta(1)SV_1R_{SR}d\tau + \frac{2}{\pi}\iint^{t} g_\alpha(2)C_1R_{PR}\left(\frac{2}{pr}\right)d\tau dt + \frac{2}{\pi}\iint^{t} g_\beta(2)SV_1R_{SR}\left(\frac{2}{pr}\right)d\tau dt + \frac{2}{\pi}\iint^{t} g_\beta(2)SH_1\left(\frac{-2}{r}\right)d\tau dt \quad (24)$$

and

$R_{PR} = -p$, $R_{SR} = \eta_\beta$ for whole space and given by expression (18) for a receiver on a free surface. Similar expressions for the dip-slip result are obtained by changing the n to 1 and the factor in parentheses reduced by two.

The 45° dip-slip result is simply

$$Q_3(r,z,\theta,t) = \frac{2}{\pi}\int^{t} g_\alpha(1)C_3R_{PR}dt + \frac{2}{\pi}\int^{t} g_\beta(1)SV_3R_{PR}d\tau \quad (25)$$

Thus, to obtain the full solution requires 26 integrations for each time step which can be compared with numerical results obtained from closed form whole space solutions in spherical coordinates. Furthermore,

the expressions in cylindrical coordinates are poorly behaved at small values of r as we will see in the numerical results discussed in the next section.

Numerical Results

In this section we will present numerical evaluations based on the formalism presented earlier for models appropriate for shallow earthquakes. However, before these equations can be applied we must specify the unknown function, D(t), the slip history or the dislocation across the fault. Although there have been many proposed slip histories we will use the one suggested by Ohnaka (1973) defined by

$$D(t) = \begin{cases} \left[1-(1+k_T t)e^{-k_T t}\right] & t > 0 \\ 0 & t < 0 \end{cases}$$

with the far field given by

$$\dot{D}(t) = k_T^2 t e^{-k_T t}$$

because of its simplicity and its similarity to the Brune (1970) far-field source. The arbitrary constant k_T will be set at 1 and 10 to simulate a relatively large earthquake, M > 7, and a moderate size, M < 6. We assumed the seismic moment to be

$$M_o = 4\pi\rho_o \times 10^{23} = 3.4 \times 10^{24} \text{ ergs}$$

which is appropriate for the smaller event and the amplitudes will be expressed in cm. For earth models, we chose a whole space, a half space, and a layer over a halfspace to keep the complexity at a minimum, but still test some commonly held assumptions, see Table 1. That is, a number

of authors have modeled local earthquakes by reducing the amplitudes of these observations by two and assuming that the earth is a whole space, see for example Trifunac (1974).

TABLE 1

Model Parameters

Layer	Thickness km	P-Velocity km/s	S-Velocity km/s	Density g/cm^3
1	2.	4.5	2.8	2.6
2	8.	6.2	3.5	2.7

As mentioned earlier the expressions in cylindrical coordinates become unstable at small r's since the near field P wave response grows rapidly and is mostly cancelled by the SV wave. This means the numerical answer is the difference of large numbers, an unpleasant situation. For this reason and to test the heavy algebra we computed the whole space response in two ways. First, by evaluating the solution in spherical coordinates, given by Harkrider (1976), and rotating the vectors into the directions r, z, and θ. The results are given on the right of Figure 2, with the corresponding solution in cylindrical coordinates, expressions (20), (22), and (24), given on the left. The short period results are identical, but the larger periods are somewhat off. Similar synthetics at larger ranges, Λ = 16 and 32 km, are identical for the short and long periods since the near-field blow up is not so severe.

In Figure 3 we display the tangential results, V, for the whole space on the right, half space in the middle, and the asymptotic on the left. As might be expected the comparison between the whole space and half space is quite good using the factor of two adjustment although there is some distortion caused by the Rayleigh pole. On the other hand, the asymptotic solution is adequate at the largest range for the short periods since most instruments would not detect the long period precursor. The only significant difference between the strike-slip and the dip-slip results is caused by the radiation pattern.

The corresponding comparisons for the vertical and radial components are given in Figures 4 and 5. For these components the factor of two, free surface adjustment, is adequate at $\Delta = 8$, but at larger ranges the diffracted P complicates the situation. On the other hand, the comparison between the full and asymptotic solutions is quite good for the short periods and even the long periods except for the strike-slip radial components at $\Delta = 8$, 16 km. The reason for this is given by the strong near-field dependence for this particular component as can be seen from expression (24). The results for the 45° dip-slip case are similar to those in Figure 5 with the comparison between asymptotic and exact being slightly better because of the smaller order number of the Bessel functions.

Actually, it is somewhat fortuitous that the asymptotic solution performs as well as it does, in that the full evaluation of the far-field term gives a poorer approximation to the full solution. The reason is that the so-called far-field term contains near-field information due to the unnatural (r) expansion. Thus, the far-field term grows rapidly in time

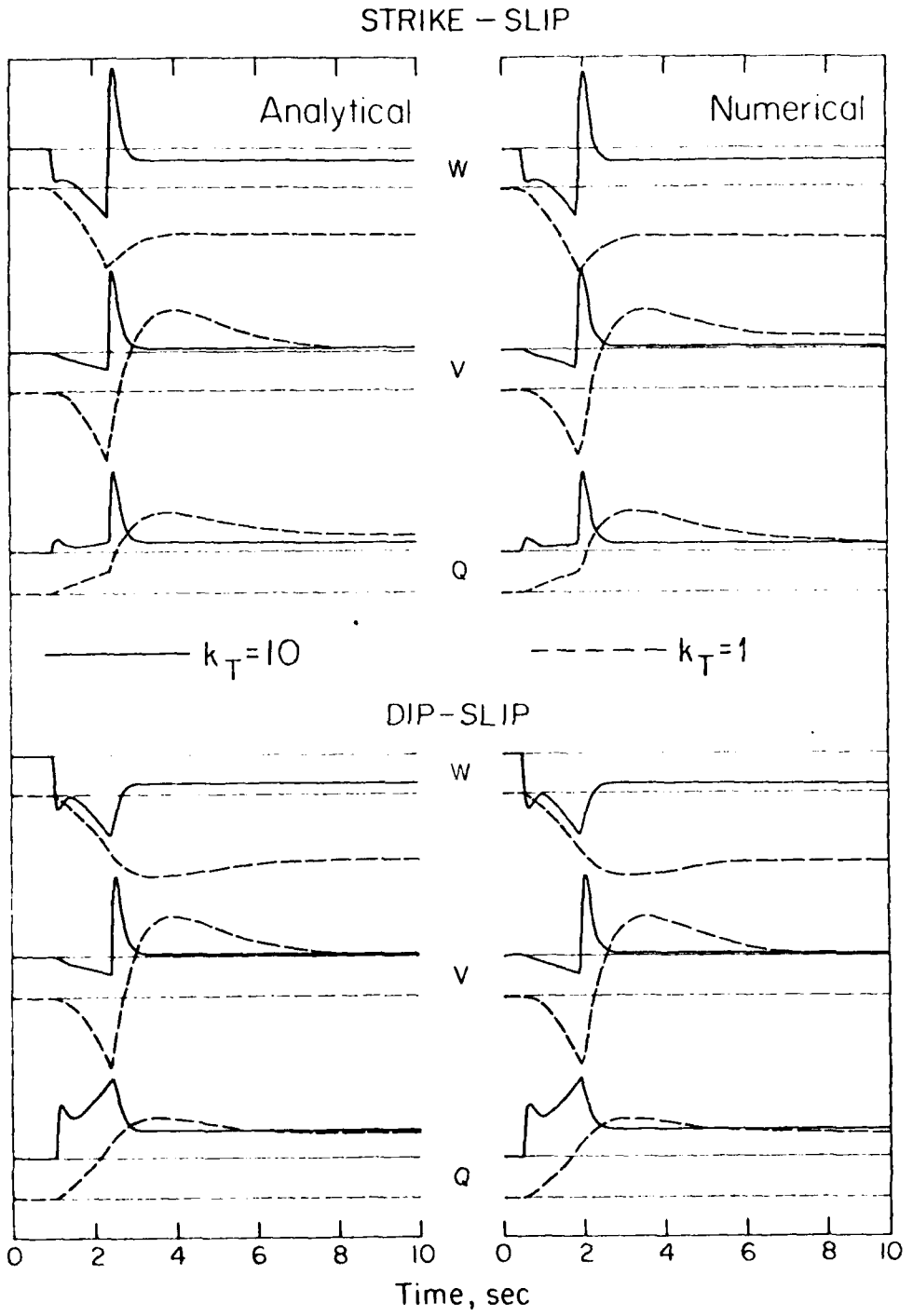

Figure IV-2. Comparison of the whole space numerical results (Cagniard - de Hoop) with the analytical results. The model parameters are specified by the half-space given in Table 1 with the top layer removed. The amplitudes along each row are the same and given explicitly in Figures 3, 4, and 5.

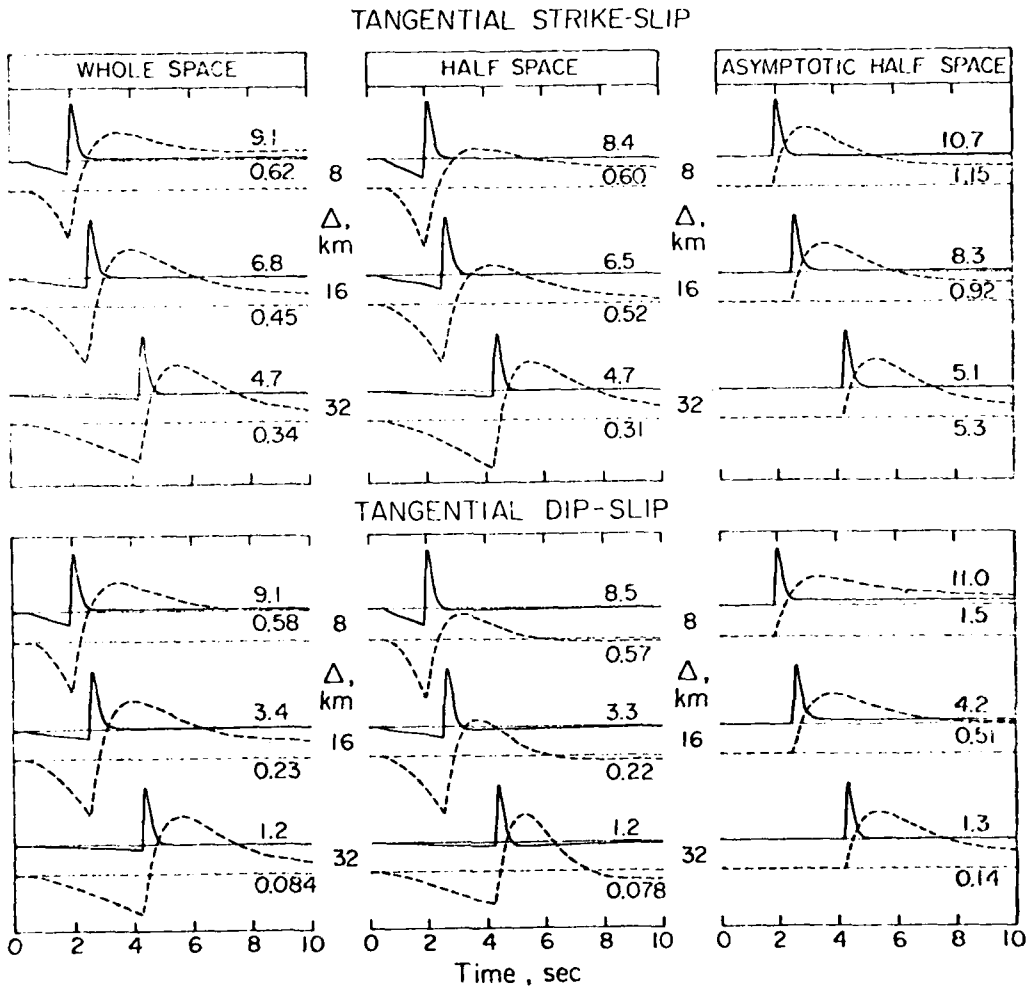

Figure IV-3. Comparison of the full Cagniard tangential response displayed on the left and middle with the asymptotic results on the right. The peak amplitude in cm is given for each trace with the whole space results doubled. Model parameters are specified by the half-space in Table 1 with the top layer removed.

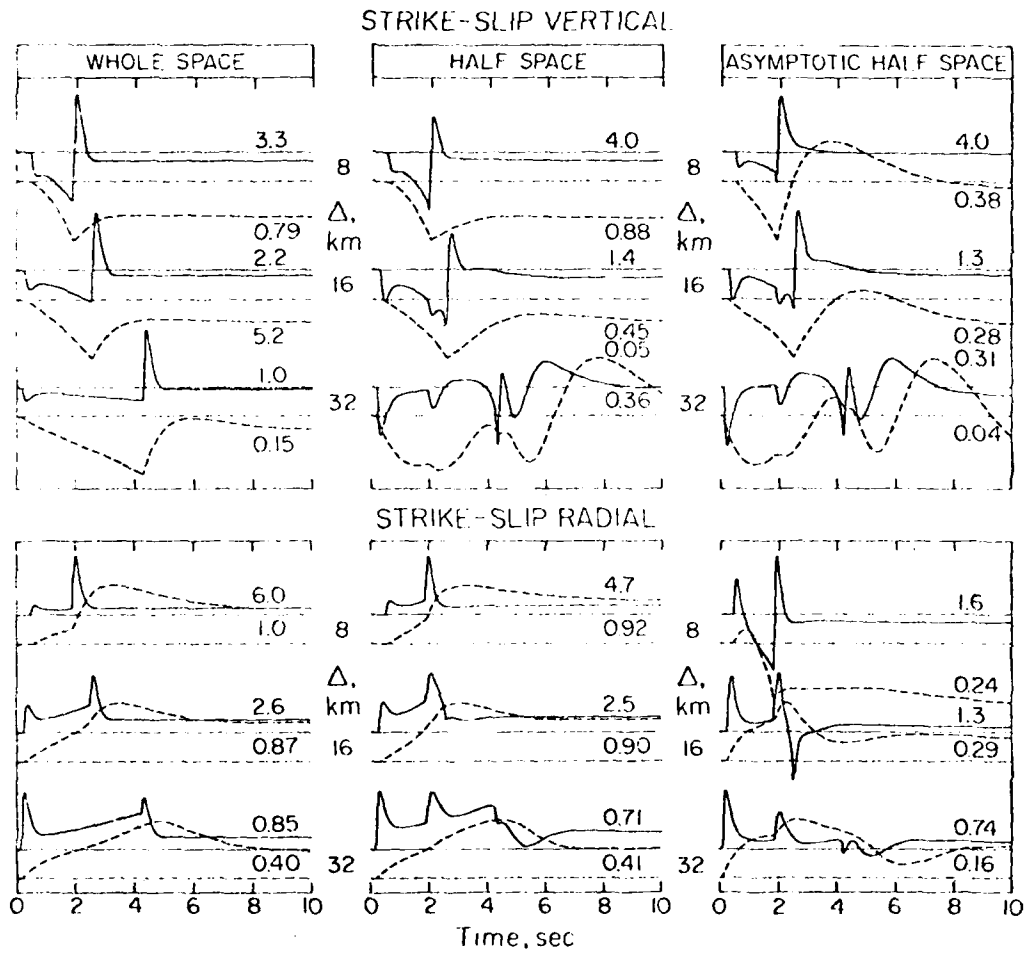

Figure IV-4. Vertical and radial comparisons for the strike-slip orientation.

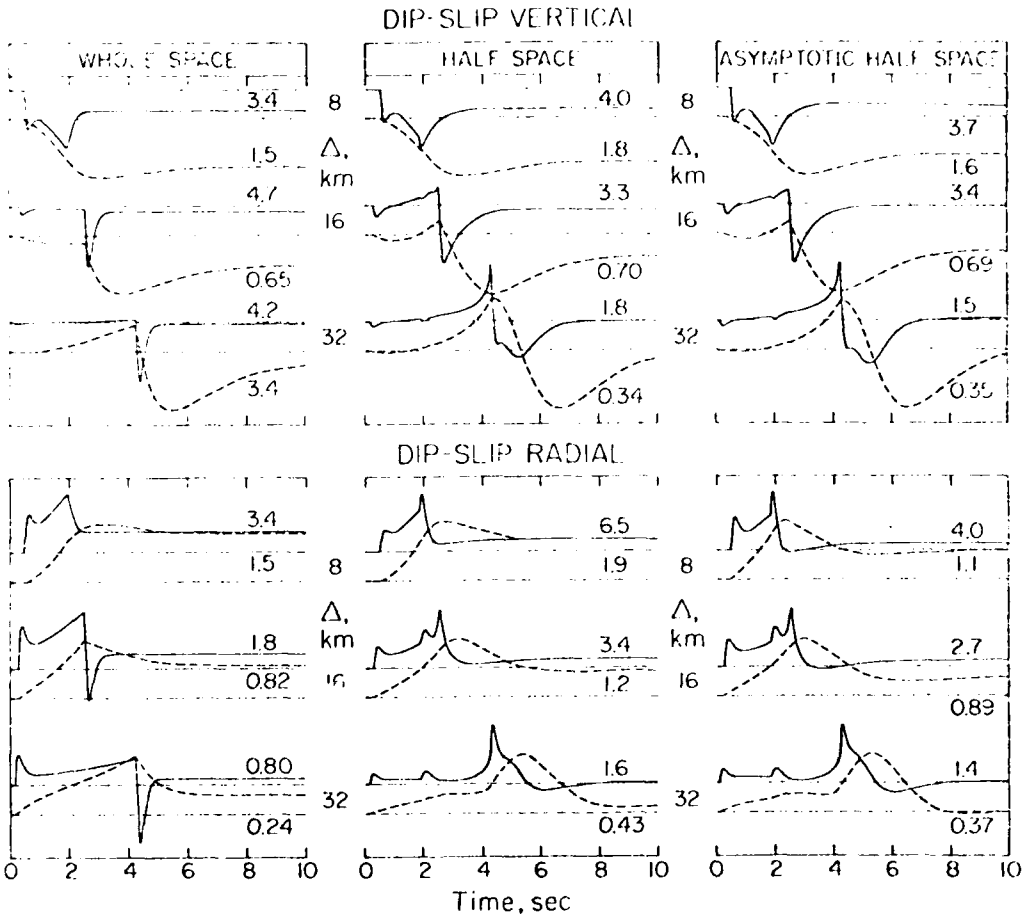

Figure IV-5. **Vertical and radial comparisons for the dip-slip orientation.**

only to be partially cancelled by the explicit near-field term of another wave type.

The comparison between the asymptotic solution and the exact can be greatly improved at the larger ranges by including higher order terms, for example see Figure 6. This solution does quite well already at r = 16 km with the results for other orientations being nearly identical with the exact after summing two terms. On the other hand, the short period results at r = 8 km for the strike-slip case are better than those presented in Figure 4, but the longer period results are not. This is the normal behavior of asymptotic solutions, but in this situation the convergence criteria is complicated by the cancellations between the various wave types as mentioned earlier.

The general agreement between the full and asymptotic solution that occurs in Figures 4 and 5 also carries over into the layered model as displayed in Figure 7. The full Cagniard solution was generated by adding up rays where the integration process must be performed on each ray separately. Thus, the computation time is much longer than for the asymptotic solution which sums the rays before performing the convolution.

Fortunately, we generally do not need many rays at small ranges because the internal reflections are also small and the exact formalism can be applied. At larger ranges, where many rays are required to model the wave guide effects, we can use the asymptotic formulation.

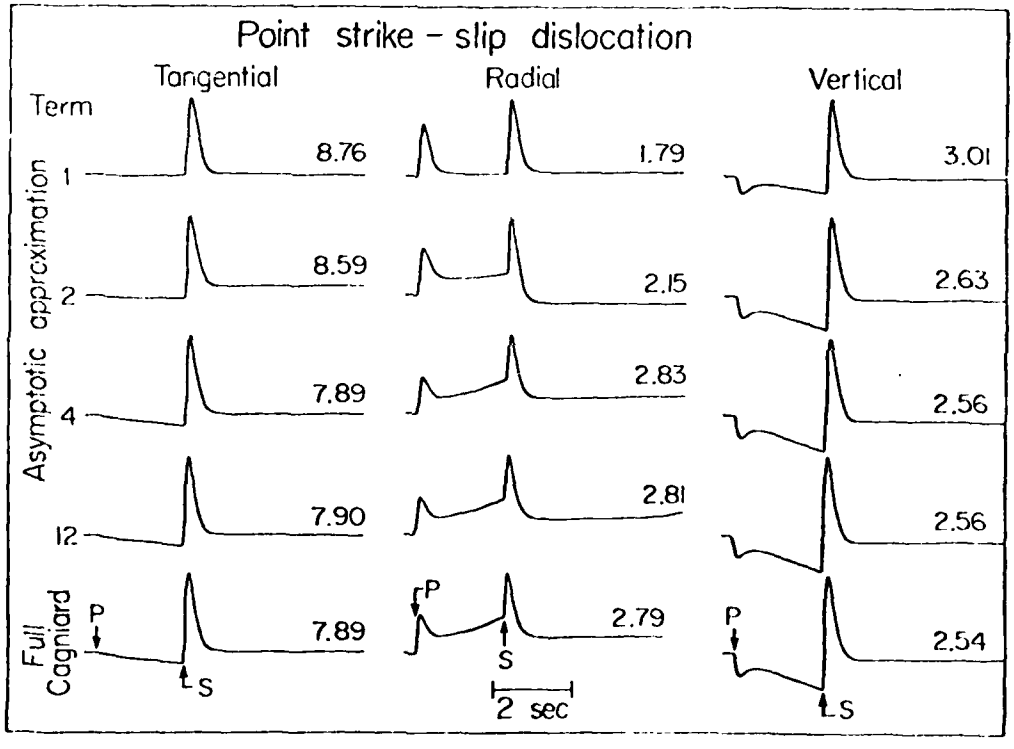

Figure IV-6. Comparison of the various components of motion for a strike-slip orientation at Λ = 16 km for a whole space. The top four rows contain the asymptotic summation after 1, 2, 4, and 12 terms. The full solution is displayed on the bottom.

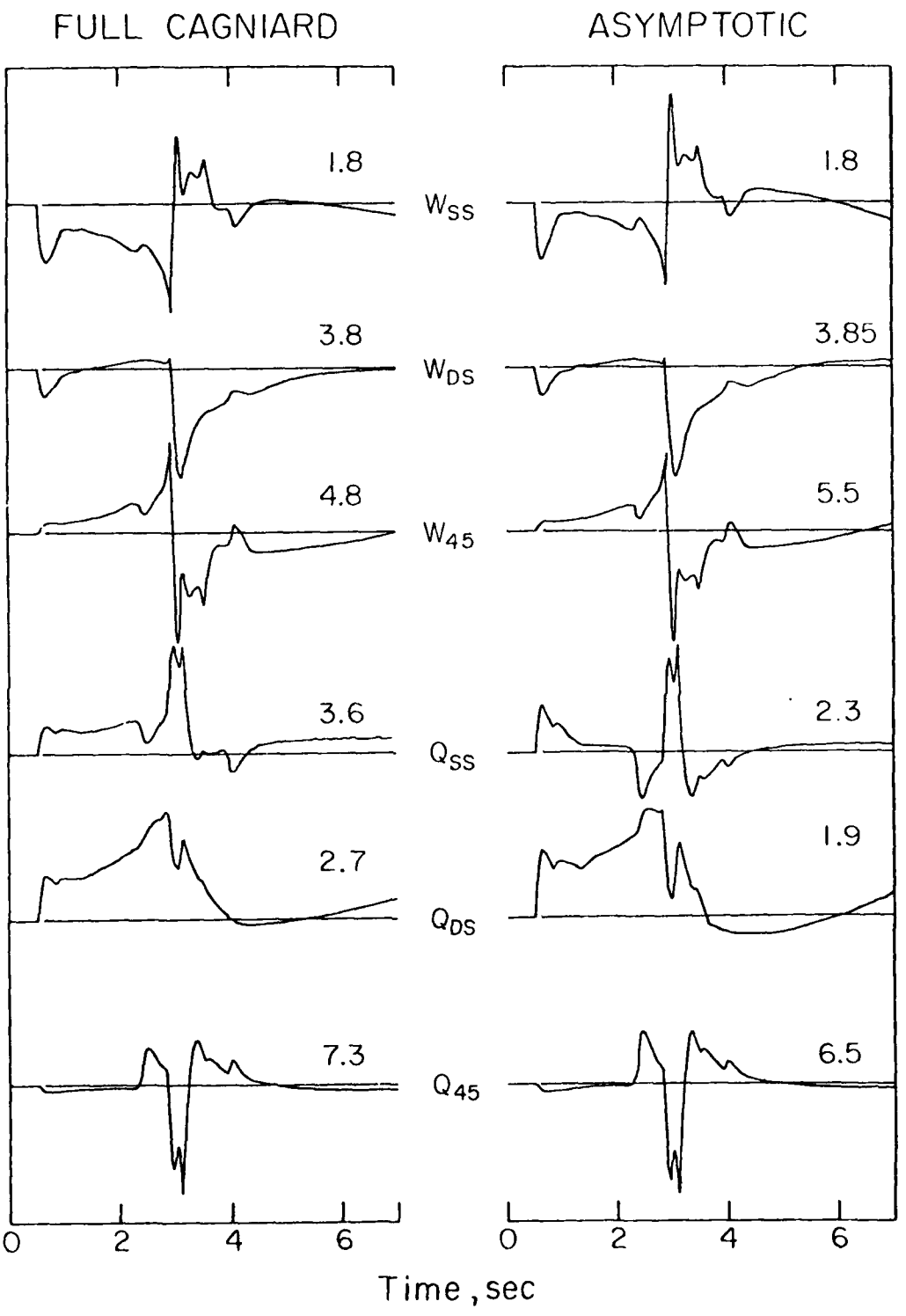

Figure IV-7. Comparison of the full solution with the asymptotic results (first term only) for a layer over a half-space model given in Table 1.

An example application of the above asymptotic technique to earthquake modeling is given in Figure 8. The observed displacement is from a strike-slip earthquake of magnitude 5 occurring in the Imperial Valley, California. This event was located in a region of known velocity structure given at the top of the figure. The only unknown parameters were the source depth and slip history, D(t), assuming the source can be simulated by a point. After a diligent search the source depth of 6.9 km and a $\dot{D}(t)$ specified by a triangular pulse with duration of 1.5 seconds was found to give the best fit, see Heaton and Helmberger (1977) for details and a discussion of the other components. A similar study was conducted on a larger earthquake, the Borrego Mountain event, where the fault was replaced by a distribution of shear dislocations (Heaton and Helmberger, 1976). Both of these studies involved observations at considerable distances, 30 and 60 km respectively, where the first term of the asymptotic solution was assumed appropriate. However, because of the large numbers of strong-motion instruments presently being deployed we will probably obtain close-in observations of a large earthquake in the near future, and thus the usefulness of the modeling procedure presented.

Acknowledgements

This research was supported by the the Earth Sciences Section, National Science Foundation Grant No. ENV76-10506 and by the Advanced Research Projects Agency of the Department of Defense and was monitored by the Air Force Office of Scientific Research under Contract No. F49620-77-C-0022.

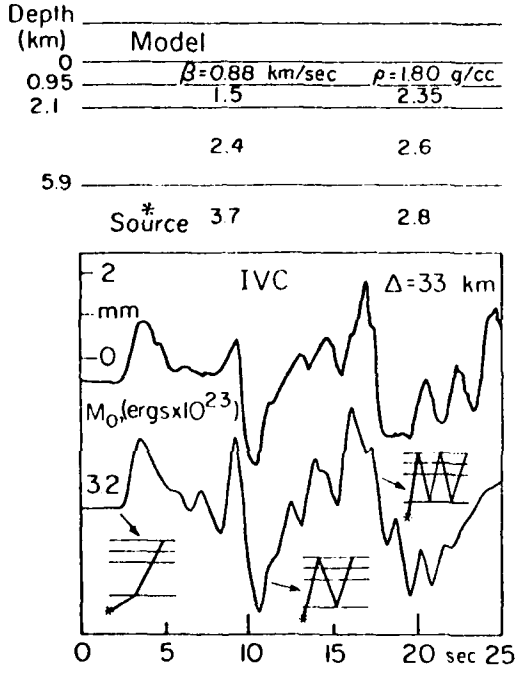
Depth (km)
Model
0
0.95
2.1
β=0.88 km/sec
ρ=1.80 g/cc
1.5
2.35
2.4
2.6
5.9
Source
3.7
2.8
2
mm
0
IVC
Δ=33 km
M0(ergs×10^23)
32
0
5
10
15
20 sec 25

Figure IV-8.

REFERENCES

Ben-Menahem, A. and M. Vered (1973). Extension and interpretation of the Cagniard-Pekeris method for dislocation sources, Bull. Seism. Soc. Am., 63, 1611-1636.

Brune, J. N. (1970). Tectonic stress and the spectra of seismic waves from earthquakes, J. Geophys. Res., 75, 4997-5009.

De Hoop, A. T. (1958). Representation theorems for the displacement in an elastic solid and their application to elastodynamic diffraction theory, Thesis, Techrische Hogeschool, Delft.

De Hoop, A. T. (1960). A modification of Cagniards method for solving seismic pulse problems, Appl. Sci. Res., B, 8, 349-356.

Gilbert, F. J. and D. V. Helmberger (1972). Generalized ray theory for a layered sphere, Geophys. J., 27, 57-80.

Harkrider, D. G. (1976). Potentials and displacements for two theoretical sources, Geophys. J., 47, 97-133.

Harkrider, D. G. and D. V. Helmberger (1978). A note on non-equivalent quadrupole source cylindrical shear potentials which give equal displacements, Bull. Seism. Soc. Am., in press.

Haskell, N. A. (1964). Total energy and energy spectral density of elastic wave radiation from propagating faults, Bull. Seism. Soc. Am., 54, 1811-1831.

Heaton, T. H. and D. V. Helmberger (1977). A study of the strong ground motion of the Borrego Mountain, California, Earthquake, Bull. Seism. Soc. Am., 67, 315-330.

Heaton, T. H. and D. V. Helmberger (1977). Predictability of strong ground motion in the Imperial Valley: Modeling the M=4.9, Nov. 4, 1976 Brawley Earthquake, Bull. Seism. Soc. Am., in press.

Helmberger, D. V. (1968). The crust-mantle transition in the Bering Sea, Bull. Seism. Soc. Am., 58, 179-214.

Helmberger, D. V. (1974). Generalized ray theory for shear dislocations, Bull. Seism. Soc. Am., 64, 45-64.

Helmberger, D. V. and S. D. Malone (1975). Modeling local earthquakes as shear dislocations in a layered half-space, J. Geophys. Res., 80, 4881-4888.

Kawasaki, I., Y. Suzuki, and R. Sato (1973). Seismic waves due to a shear fault in a semi-infinite medium, J. Phys. Earth, 21, 251-284.

Knopoff, L., R. W. Fredricks, A. F. Gangi, and L. P. Porter (1957). Surface amplitudes of reflected body waves, Geophysics, 22, 842-847.

Lamb, H. (1904). On the propagation of tremors over the surface of an elastic solid, Phil. Trans. Roy. Soc. London, A203, 1-42.

Langston, C. A. and D. V. Helmberger (1975). A procedure for modeling shallow dislocation sources, Geophys. J. R. Astr. Soc., 42, 117-130.

Ohnaka, M. (1973). A physical understanding of the earthquake source mechanism, J. Phys. Earth, 21, 39-59.

Pekeris, D. L. (1940). A pathological case in the numerical solution of integral equations, Proc. Nat'l Acad. Sci., U.S., 26, 433-437.

Spencer, T. (1960). The method of generalized reflection and transmission coefficients, Geophysics, 25, 625-641.

Trifunac, M. D. (1974). A three-dimensional dislocation model for the San Fernando, California, Earthquake of February 9, 1971, Bull. Seism. Soc. Am., 64, 149-172.

V. Theoretical and Block Conversion of Explosion P Waves into SH and SV Waves

C. Salvado and J. B. Minster

For the purpose of investigating the possible generation of S waves by purely dilational sources in a jointed medium, we have been led to consider a new category of boundary conditions. The concept of joint movement and block motions forces us to abandon the concept of welded interfaces with continuous displacements. Since we are principally interested in the generation of shear waves, we keep the normal component of displacement continuous across the interface, but allow the tangential component to be discontinuous. The design of a suitable boundary condition requires that we link the jump in tangential displacement to the tractions along the interface, which must themselves be continuous since no layer of body forces is introduced.

In order to keep the problem manageable, and to derive analytical solutions, we have adopted a linear boundary condition whereby the jump of tangential velocity is directly proportional to the shear traction across the interface, so that

$$\left[\bar{t}_T\right] = \frac{\phi}{1-\phi}\,\frac{\mu}{\beta}\left[\dot{u}_T\right] \quad ; \quad 0 \leq \phi < 1$$

where t_T is the tangential component of traction $\dot{u}_T$ the tangential component of velocity; μ, β are the rigidity and shear velocity respectively, introduced here for homogeneity, and assumed to be the same as both sides of the interface - ϕ is termed the bonding parameter; for $\phi = 0$ the tangential traction vanishes and the interface is perfectly lubricated; for $\phi = 1$, the jump in

velocity must vanish and the interface is perfectly bonded such. Such a boundary condition has been used by Murty (1975, 1976).

This boundary condition, although very simple, possesses a number of desirable properties. It allows conversion of P and SV waves even in the case where the interface separates identical elastic half spaces; Murty found that in the case of the reflection and refraction of plane waves, this boundary constitutes an energy sink. This can hold physically only in the limit of wavelengths long compared to the thickness of the physical joint, which explains the lack of a characteristic time scale in the problem. The absence of such a characteristic time, and thus of a characteristic frequency permits us to treat the wave propagation problem using the Cagniard-de Hoop technique.

To investigate and illustrate the properties of such an interface, we take the interface to be vertical, and consider a purely compressional (explosive) source at a short distance h from it. We restrict ourselves to rays in a horizontal plane containing the source (i.e. with a take-off angle of 90°). Any S wave polarized in that plane will be a pure SH wave by definition. The wave propagation problem is solved using a high frequency first motion approximation; we present the results for a unit step source function, and for several values of the bonding parameter ϕ.

Figure 1 illustrates the geometry; we shall ignore for the moment wave interactions with the free surface so that the problem has radial symmetry about OZ. Figure 2 shows the peak displacement jump as a function of radial distance r, for various bondings. It is clear that values of ϕ much greater than .5 greatly limit the relative displacement across the interface, so that we expect wave conversion to be most efficient for low ϕ.

Figure 3 depicts the radiation pattern of SH waves in the (z, x) plane, for a perfectly lubricated interface. This is a form lobed pattern which exhibits very large amplitudes along directions which correspond to critical reflections. A similar phenomena was found by Burridge et al. (1964) in the case of a free surface. As can be seen on Figures 4 and 5, the radiation pattern changes shape with increasing ϕ; this variation is probably too subtle, however, to be observable in the field. Much more significant, on the other hand, is the large drop in amplitude as ϕ increases. For $\phi = .5$, the largest SH amplitude is only 1/10 of the incident P wave, this ratio drops to 1/100 for $\phi = .9$.

The amplitudes plotted on these figures are measured perpendicular to a ray joining the source S to the receiver. Since the source is actually at a distance h from the interface where wave conversion takes place, there exists a parallax effect, and thus a component of "radial" motion associated with the converted S wave. This component is plotted as a dotted line on the figures.

It appears, therefore, that it is possible to generate SH radiation in the earth by detonating an explosive source near a vertical joint across which differential slip is allowed to occur. This mechanism does not require the existence of regional prestress, but will, in general, be quite inefficient unless the joint is fairly well lubricated. It must be noted that although the SH amplitude radiation pattern show a certain resemblance with double couple radiation patterns, the phase is quite different. In these figures the phases are antisymmetric about the interface, and are symmetric about the X axis, perpendicular to the interface. Further inferences about S wave generation using such a mechanism must await further calculations; in particular, crucial problems are the generation of Love waves, and the behavior of such interfaces limited in space.

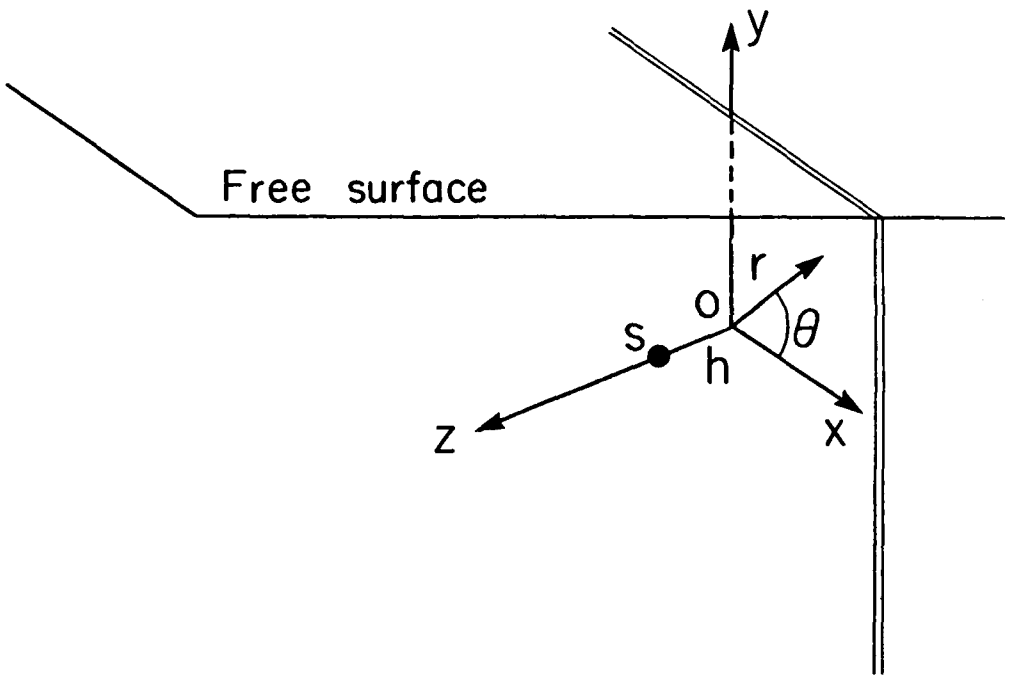

Figure V-1

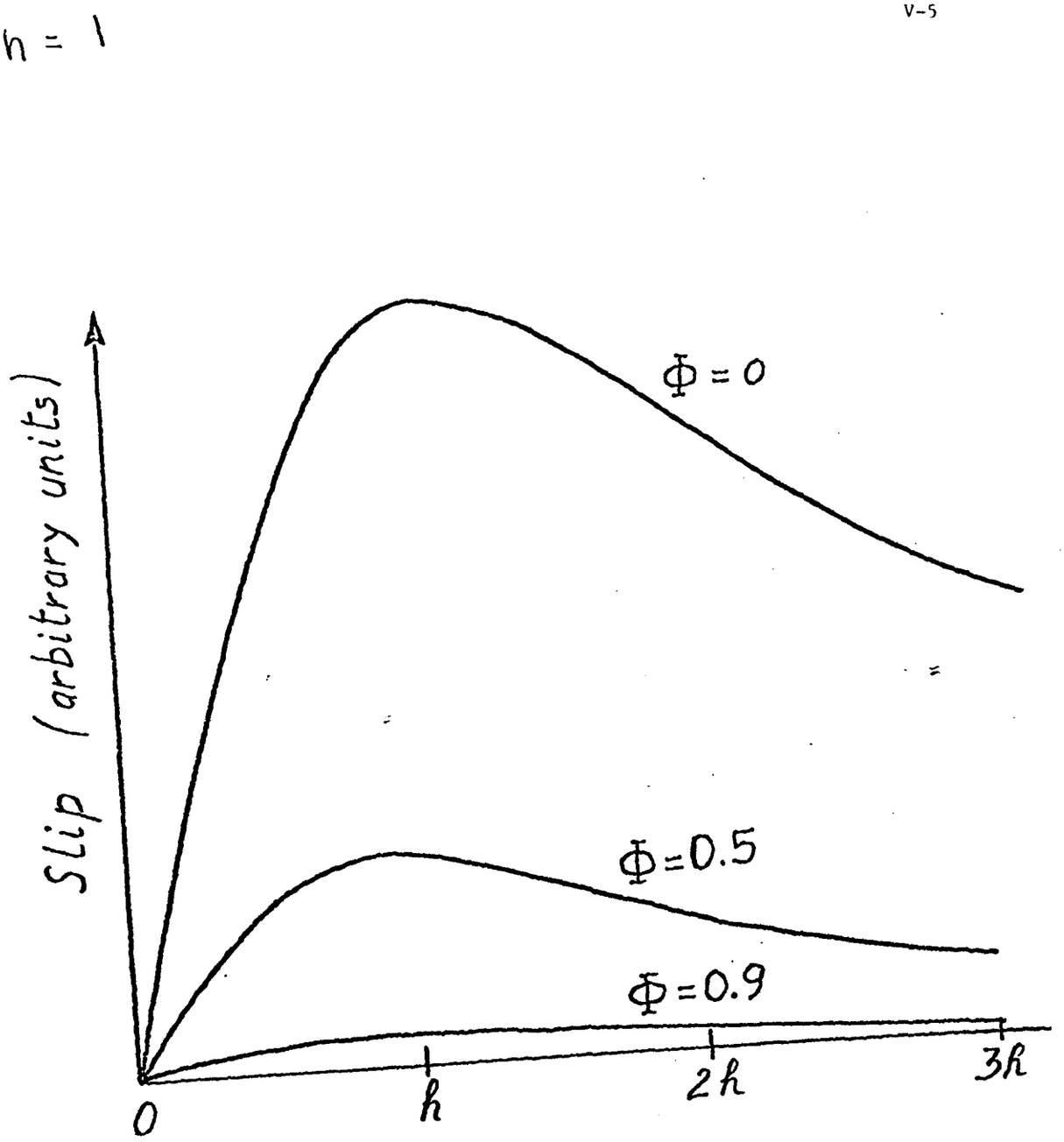

Figure V-2

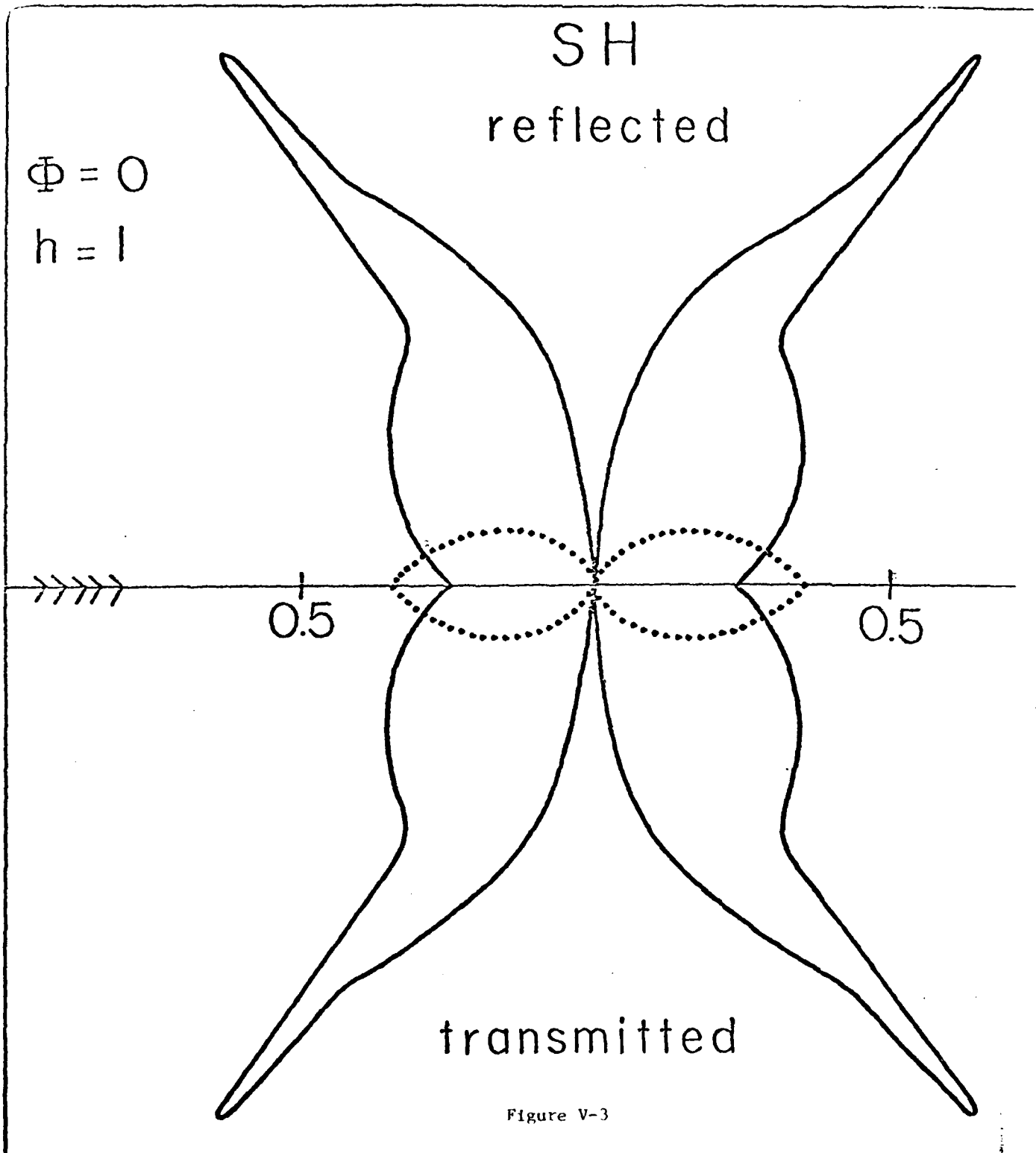

Figure V-3

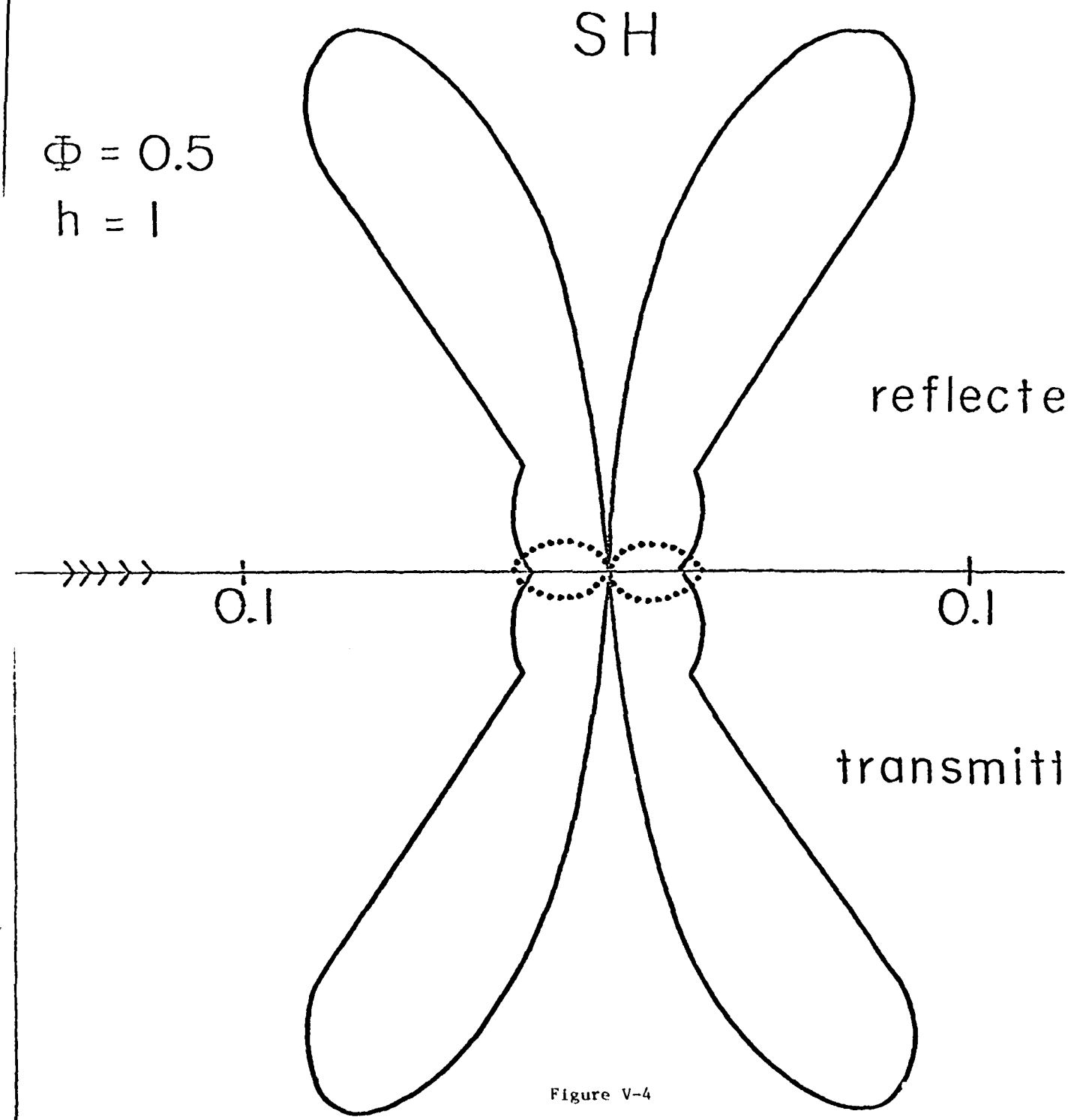

Figure V-4

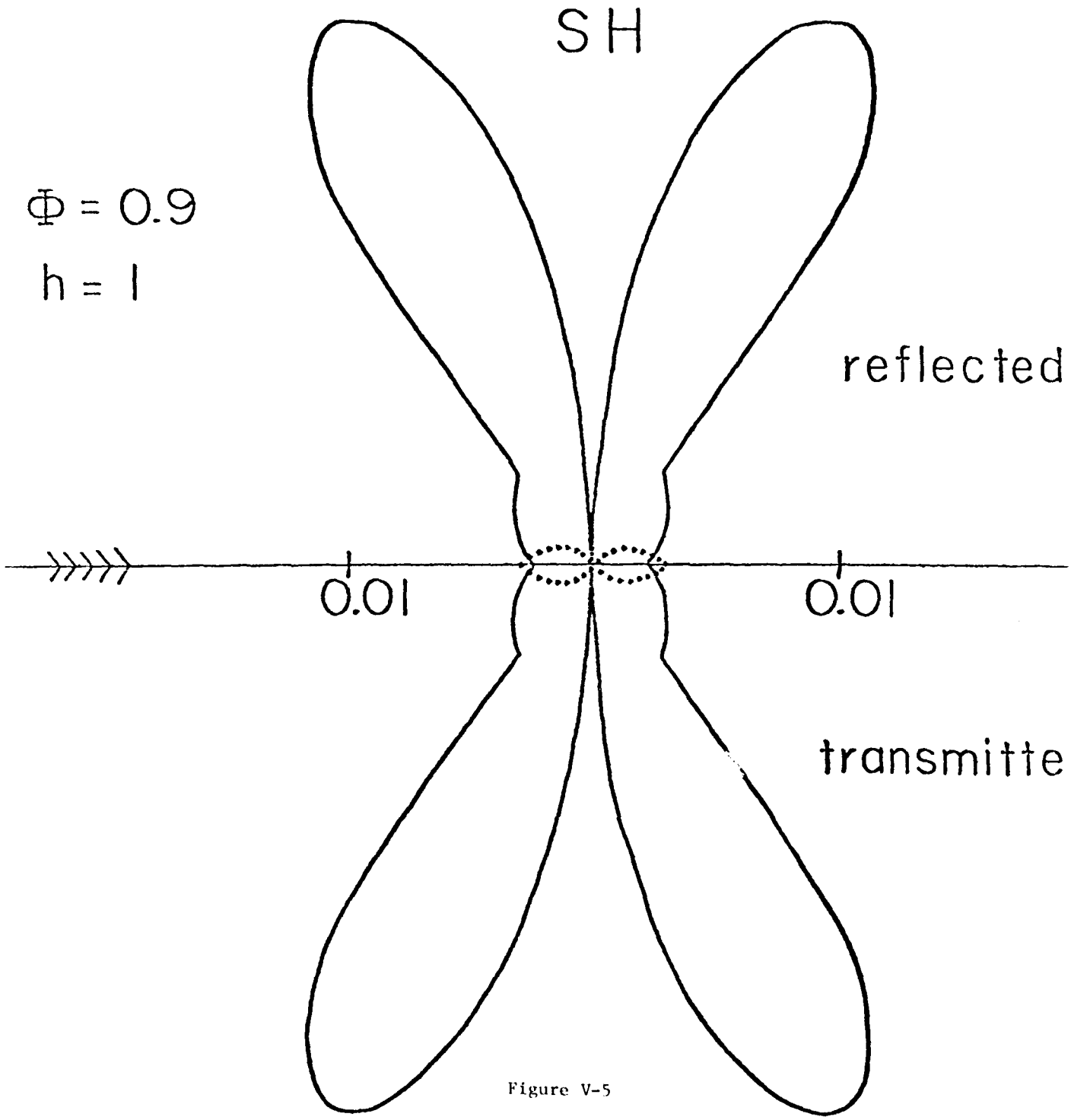

Figure V-5

VI. Publications

Previous Technical Reports

10/1/76 - Present

Bache, T. C., and Harkrider, D. G., 1976, The body waves due to a general seismic source in a layered earth model: 1. Formulation of the theory: Seismol. Soc. America Bull., v. 66, p. 1805-1819.

Anderson, D. L., and Hart, R. S., 1976, Absorption and the low-velocity zone: Nature, v. 263, p. 397-398.

Geller, R. J., 1976, Body force equivalents for stress drop seismic sources: Seismol. Soc. America Bull., v. 66, p. 1801-1804.

Harkrider, D. G., 1976, Potentials and displacements for two theoretical seismic sources: Geophys. J. R. astr. Soc., v. 47, p. 97-133.

Minster, J. B., 1976, Transformation of multipolar source fields under a change of reference frame: Geophys. J. R. astr. Soc., v. 47, p. 397-409.

Hart, R. S., Butler, Rhett, and Kanamori, Hiroo, 1976, Surface-wave constraints on the August 1, 1975 Oroville earthquake: Seismol. Soc. America Bull., v. 67, p. 1-7.

Liu, H. P., Anderson, D. L., and Kanamori, Hiroo, 1976, Velocity dispersion due to anelasticity; Implications for seismology and mantle composition: Geophys. J. R. astr. Soc., v. 47, p. 41-58.

Langston, C., and Butler, R., 1976, Focal mechanism of the August 1, 1975, Oroville earthquake: Seismol. Soc. America Bull., v. 66, p. 1111-1120.

Chung, W. Y., and Kanamori, Hiroo, 1976, Source process and tectonic implications of the Spanish deep focus earthquake of March 29, 1954: Phys. Earth and Planet. Int., v. 13, p. 85-96.

Helmberger, D. V., 1977, Fine structure of an Aleutian crustal section: Geophys. J. R. astr. Soc., v. 48, p. 81-90.

Kanamori, Hiroo, and Anderson, D. L., 1977, Importance of physical dispersion in surface wave and free oscillation problems: Review: Rev. of Geophys. and Space Phys., v. 15, p. 105-112.

Langston, C. A., 1977, Corvallis, Oregon, crustal and upper mantle receiver structure from teleseismic P and S waves: Seismol. Soc. America Bull., v. 67, p. 713-724.

Helmberger, D. V., and Johnson, Lane, 1977, Source parameters of moderate size earthquakes and the importance of receiver crustal structure in interpreting observations of local earthquakes: Seismol. Soc. America Bull., v. 67, p. 301-313.

Geller, R. J., and Kanamori, Hiroo, 1977, Magnitudes of great shallow earthquakes from 1904 to 1952: Seismol. Soc. America Bull., v. 67, p. 557-598.

Anderson, D. L., Kanamori, Hiroo, Hart, R. S., and Liu, H. P., 1977, The earth as a seismic absorption band: Science, v. 196, p. 1104-1106.

Hill, D. P., and Anderson, D. L., 1977, A note on the earth stretching approximation for Love Waves: Seismol. Soc. America Bull., v. 67, p. 551-552.

Harkrider, D. G., 1977, Elastic relaxation coefficients for a spherical cavity in a prestressed medium of arbitrary orientation: Geophys. J. R. astr. Soc., v. 50, p. 487-491.

Hart, R. S., Anderson, D. L., and Kanamori, Hiroo, 1977, The effect of attenuation on gross earth models: Jour. Geophys. Research, v. 82, p. 1647-1654.

Anderson, D. L., 1977, Composition of the mantle and core: Ann. Rev. Earth Planet. Sci., v. 5, p. 179-202.

Okal, E. A., 1977, The effect of intrinsic oceanic upper-mantle heterogeneity on regionalization of long-period Rayleigh-wave phase velocities: Geophys. J. R. astr. Soc., v. 49, p. 357-370.

Minster, J. B., and Suteau, A. M., 1977, Far-field waveforms from an arbitrarily expanding, transparent spherical cavity in a prestressed medium: Geophys. J. R. astr. Soc., v. 50, p. 215-233.

Langston, C. A., and Blum, D. E., 1977, The April 29, 1965, Puget Sound earthquake and the crustal and upper mantle structure of western Washington: Seismol. Soc. America Bull., v. 67, p. 693-711.

Kanamori, Hiroo and D. L. Anderson, 1977, Importance of physical dispersion in surface wave and free oscillation problems: review. Rev. Geophys. Space Phys., 15, no. 1, 105-112.

Heaton, T. H. and Helmberger D. V., 1977, A study of the strong ground motion of the Borrego Mountain, California, earthquake: Seismol. Soc. America Bull., v. 67, no. 2 p. 315-330.

Butler, Rhett, 1977, A Source of Bias in Multiple ScS Differential Travel Times Determined by Waveform Correlation: Geophysical Research Letters, v. 4, no. 12, p. 593-595.

Hong, T.L. and Helmberger D. V., 1977, Generalized Ray Theory for Dipping Structure: Seismol. Soc. America Bull., v., 67, no. 4, pp. 995-1008.

Harkrider, D. G., and Helmberger, D. V., 1978, A note on non-equivalent quadrupole source cylindrical shear potentials which give equal displacements: Seismol. Soc. America Bull., in press.

Anderson, D. L., and Hart, R. S., 1978, Attenuation models of the earth: Phys. Earth and Planet. Int., in press.

Burdick, L. J., and Helmberger, 1978, The upper mantle P velocity structure of the western United States: Jour. Geophys. Research, in press.

Minster, J. B., 1978, Transient and impulse responses of a one-dimensional linearly attenuating medium; Part 1: Analytical results: Geophys. J. R. astr. Soc., in press.

Minster, J. B., 1978, Transient and impulse responses of a one-dimensional linearly attenuating medium; Part II: A parametric study: Geophys. J. R. astr. Soc., in press.

PAPERS SUBMITTED FOR PUBLICATION

Ebel, John, Burdick, L. J., and Stewart, G. S., 1978, The source mechanism of a strike-slip earthquake in Baja California: Seismol. Soc. America Bull.

McNally, K. C., 1978, Earthquake-history reconstruction and seismicity 1936-1975: San Andreas Fault, Central California: Seismol. Soc. America Bull.

Hart, R. S., and Butler, Rhett, 1978, Shear wave travel times and amplitudes for two well-constrained earthquakes: Seismol. Soc. America Bull.

Burdick, L. J., 1978, t* for S waves with a continental raypath: Seismol. Soc. America Bull.

Minster, J. B., 1978, Near field waveforms from an arbitrarily expanding, transparent spherical cavity in the prestressed medium: Geophys. J. R. astr. Soc.

ABSTRACTS

AGU Meeting, San Francisco

December 5 - 9, 1977

Butler, R., "Lateral variation of P-wave amplitudes from Bombs: A case for variation in T*".

Hart, R. S. and R. Butler, "S wave travel times and lower mantle shear velocity from waveform correlations".

Salvado, C. and J. B. Minster, "Compressional waves incident on a loosely bonded interface of two identical solids".